

Unravelling free volume in branched-cation ionic liquids based on silicon

Eduards Bakis,^{*a} Kateryna Goloviznina,^b Inês C. M. Vaz,^b Diana Sloboda,^a Daniels Hazens,^a Valda Valkovska,^a Igors Klimenkovs,^a Agilio Padua^b and Margarida Costa Gomes^{*b}

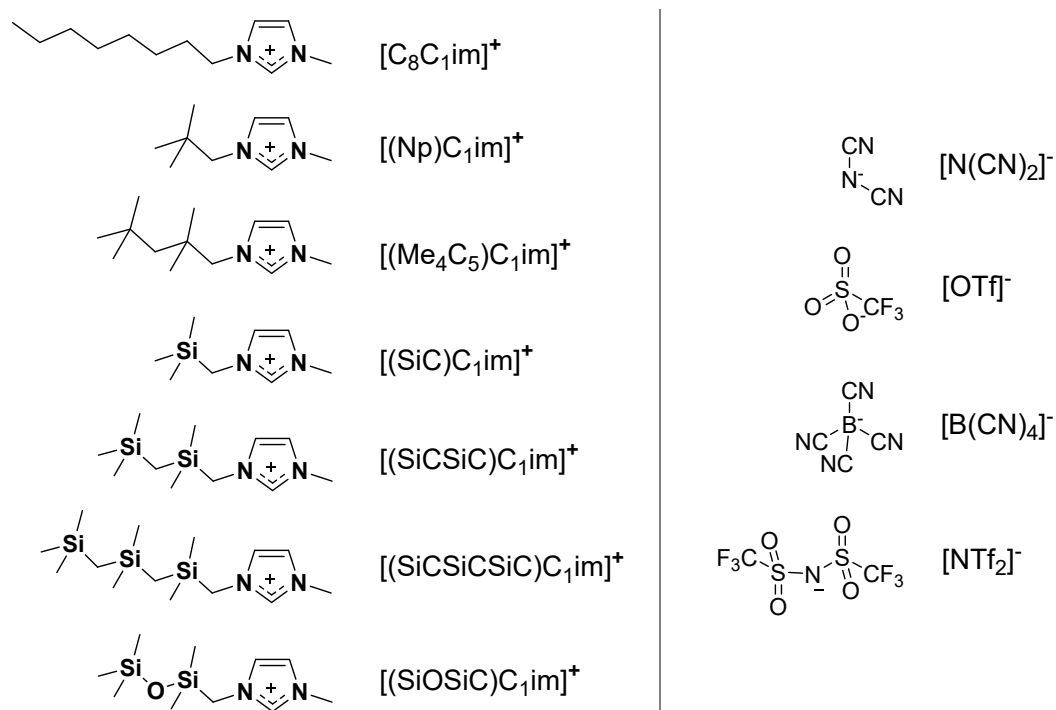
^a Faculty of Chemistry, University of Latvia, Jelgavas 1, Riga, LV-1004, Latvia

^b Laboratoire de Chimie, ENS de Lyon and CNRS, 46 allée d'Italie, 69364 Lyon, France

Electronic Supplementary Information

1. Ion structures and nomenclature for ionic liquids studied	2
2. Synthetic details	3
3. MD simulation	3
4. Analytical methods for structure determination	8
5. Synthetic procedures	8
6. High resolution mass spectra	18
7. Density fitting parameters	21
8. Ionic liquid viscosity fitting parameters	23
9. Viscosities of [(SiOSiC) ₁ im] ⁺ ionic liquids reported in literature	24
10. Gas solubility measurements	24
11. Thermodynamic properties derived from gas solubility measurements	29
12. Correlation between argon solubility and molar volume of ionic liquids	34
13. List of ionic liquid intermediates prepared according to paths a or b	34
14. Synthetic approaches for introduction of cation side-chains and anion metathesis	35
15. Bond lengths in hydrocarbons and their silicon analogue molecules	36
16. Molar volume of ionic liquids	37
References	38

1. Ion structures and nomenclature for ionic liquids studied



Scheme S1. Schematic structures and abbreviations of the anions and cations for the ionic liquids studied in this work

Table S1. List of the Ionic liquids studied on this work, the CAS registry numbers and its molecular weight (g mol^{-1}).

No	Ionic Liquid	CAS No	MW
1	$[(\text{Np})\text{C}_1\text{im}][\text{NTf}_2]$	871127-69-4	433.3908
2	$[(\text{SiC})\text{C}_1\text{im}][\text{NTf}_2]$	871127-68-3	449.4656
3	$[(\text{SiCSiC})\text{C}_1\text{im}][\text{B}(\text{CN})_4]$	-	356.3812
4	$[(\text{SiCSiC})\text{C}_1\text{im}][\text{N}(\text{CN})_2]$	-	307.5421
5	$[(\text{SiCSiC})\text{C}_1\text{im}][\text{OTf}]$	-	390.5697
6	$[(\text{SiCSiC})\text{C}_1\text{im}][\text{NTf}_2]$	-	521.6467
7	$[(\text{SiOSiC})\text{C}_1\text{im}][\text{B}(\text{CN})_4]$	-	358.3540
8	$[(\text{SiOSiC})\text{C}_1\text{im}][\text{N}(\text{CN})_2]$	-	309.5149
9	$[(\text{SiOSiC})\text{C}_1\text{im}][\text{NTf}_2]$	936638-34-5	523.6195
10	$[(\text{Me}_4\text{C}_5)\text{C}_1\text{mim}][\text{NTf}_2]$	-	489.4971
11	$[(\text{SiCSiCSiC})\text{C}_1\text{im}][\text{NTf}_2]$	-	593.8278

2. Synthetic details

1-Methylimidazole, chloromethyltrimethylsilane, lithium bis-(trifluoromethanesulfonyl)imide, lithium trifluoromethanesulfonate and sodium dicyanamide were purchased from *Fluorochem*. 1-Methylimidazole was stirred over solid KOH under argon for 24 h and distilled at reduced pressure prior to use.

Chloromethyldimethylchlorosilane was purchased from *Gelest*, stored and manipulated under argon, and used without prior purification.

Potassium trimethylsilanolate was purchased from *Acros Organics* as a 2M solution in THF.

Unless stated otherwise, all syntheses were carried out under argon using oven-dried glassware and dry solvents.

3. MD simulation

Molecular dynamics simulation of periodic cubic boxes was performed in LAMMPS¹ with USER-DRUDE² and USER-FEP packages enabled. Initial configurations were generated using Packmol,³ the input files were prepared with fftool, polarizer and scaleLJ tools available in our public repositories.^{4,5} The cut-off radius was set to 12 Å for non-bonded interactions, the tail correction was applied to energy and pressure. The electrostatic energies were computed with the particle-particle particle-mesh (PPPM) method with an accuracy of $1 \cdot 10^{-5}$. Bonds involving hydrogen atoms were constrained using the SHAKE algorithm. The temperature-grouped Nosé-Hoover thermostat and a barostat were used to maintain temperature at 353 K and pressure at 1 bar for structural analysis. We replaced the tgNH with a Langevin thermostat when evaluating free energy of gas solvation in ILs due to stability issues. The time step was of 1 fs.

Drude induced dipoles⁸ were used to account for explicit polarization effects: each atomic site was represented by a positively charged Drude core (DC) and a negatively charged Drude particle (DP) of 0.4 a.u. mass attached to the DC by a spring ($k_D = 4184$ kJ/mol). The partial charges of DPs were evaluated from atomic polarizabilities according to $\alpha = q_D^2/k_D$. Atomic polarizabilities of atoms in the ILs were taken from the recent work of Schröder.⁹ The polarizabilities of neutral Si and Ar atoms were taken from a widely used database of Schwerdtfeger,¹⁰ with the contribution of 1.87 \AA^3 subtracted from the atomic polarizability of silicon in order to account for its positive, close to unity partial charge in imidazolium-based cations.¹¹ Heavy atoms were considered as polarizable, and polarizability of hydrogen atoms were merged onto the atoms they are attached to. The Thole function^{2,12,13} was used to damp short-range interactions between the induced dipoles to avoid instabilities of simulations with the α parameter set to 2.6. In order to approximate the dynamics of the system to the self-consistent regime, Drude particles were kept at 1 K.²

The systems studied belong to the imidazolium family with alkyl, alkylsilane and siloxane side-chains, combined with bis(trifluoromethanesulfonyl)imide ([NTf₂]⁻), dicyanamide ([N(CN)₂]⁻), tetracyanoborate ([B(CN)₄]⁻) and triflate ([OTf]⁻) anions. Argon was used as solute.

The CL&Pol^{14,15} polarizable force field was used for modelling imidazolium-based cations with alkyl side chains, and also [NTf₂]⁻, [OTf]⁻ and [N(CN)₂]⁻ anions. It was extended to branched alkylsilane cationic side chain, to the TCB⁻ anion and to argon, according to the procedure developed earlier.¹⁴ The fixed-charge CL&P-based

force field of $[(\text{SiC})\text{C}_1\text{im}]^+$ and $[(\text{SiOSiC})\text{C}_1\text{im}]^+$ proposed by Castner¹⁶ was transformed into a polarizable version by adding Drude induced dipoles on each non-hydrogen atom and scaling the parameters of Lennard-Jones potential to avoid double counting of induction effects. The atomic partial charges of $[(\text{SiC})\text{C}_1\text{im}]^+$, $[(\text{SiCSiC})\text{C}_1\text{im}]^+$ and $[(\text{SiOSiC})\text{C}_1\text{im}]^+$ cations were computed using CHelpG/MP2/cc-pVTZ¹⁷ on previously optimized geometries in Gaussian.¹⁸ The coefficients in the cosine series of the Si-C-Si-C dihedral were found by fitting the difference between the *ab-initio* potential energy profile of bis(trimethylsilyl)methane in gas phase calculated at MP2/cc-pVTZ//HF/6-31G(d) level and the MD energy profile of the isolated molecule with the target dihedral coefficients set to zero (Figure S1). A detailed description of the procedure was presented in the articles on development of OPLS-AA¹⁹ and CL&P²⁰ force fields. The interactions parameters of $[\text{B}(\text{CN})_4]^-$ anion were obtained from private communication with F. Philippi (Imperial College London), and OPLS-AA fixed-charge force field²¹ served as a basis for the polarizable force field of argon.

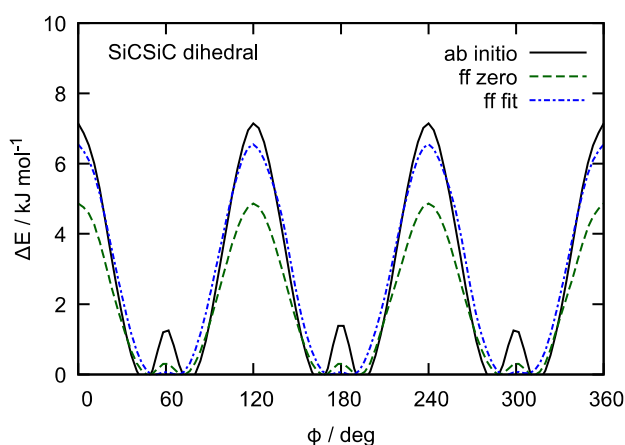


Figure S1. Torsion profile of the Si-C-Si-C dihedral in $[(\text{SiCSiC})\text{C}_1\text{im}]^+$ cation. The cosine series coefficients of are $v_1, v_2, v_4 = 0, v_3 = 0.6442$.

The scaling coefficients (Table S2) applied to the original, fixed-charge Lennard-Jones parameters²² of the interactions between fragments were evaluated using the predictive scheme.¹⁴ Imidazolium-based cations were represented by an 1,3-dimethylimidazolium ($[\text{C}_1\text{C}_1\text{im}]^+$) head group and a side chain: neopentyl (Np) for $[(\text{Np})\text{C}_1\text{im}]^+$, and $[(\text{Me}_4\text{C}_5)\text{C}_1\text{im}]^+$; tetramethylsilane (TMS) for $[(\text{SiC})\text{C}_1\text{im}]^+$ and $[(\text{SiCSiC})\text{C}_1\text{im}]^+$; hexamethyldisiloxane ($(\text{SiC})_2\text{O}$) for $[(\text{SiOSiC})\text{C}_1\text{im}]^+$. Only linear 3-methyl-1-octylimidazolium was represented by 1-ethyl-3-methylimidazolium $[\text{C}_2\text{C}_1\text{im}]^+$ and butane (C_4H_{10}) fragments to be consistent with previous works.¹⁴ The $[\text{NTf}_2]^-$, $[\text{N}(\text{CN})_2]^-$, $[\text{B}(\text{CN})_4]^-$, $[\text{OTf}]^-$ anions and argon were treated as entire fragments. The Lennard-Jones diameters of atoms in ions were decreased by 1.5% in order to correct density values.¹⁴

Table S2. Scaling coefficients for the modification of non-bonded attractive interactions

Fragment <i>i</i>	Fragment <i>j</i>	k_{ij}	IL(s)
Ar	$[C_1C_1im]^+$	0.78	all branched cation ILs
	$[C_2C_1im]^+$	0.80	$[C_8C_1im][NTf_2]$
	$[NTf_2]^-$	0.72	$[Cat][NTf_2]$
	$[DCA]^-$	0.72	$[(SiCSiC)C_1im][DCA]$
	$[B(CN)_4]^-$	0.77	$[(SiCSiC)C_1im][B(CN)_4]$
	$[OTf]^-$	0.47	$[(SiCSiC)C_1im][OTf]$
	TMS	1.00	$[(SiC)C_1im][NTf_2]$; $[(SiCSiC)C_1im][Ani]$
	Np	1.00	$[(Np)C_1im]$, $[(Me_4C_3)C_1im]$ $[NTf_2]$
	C_4H_{10}	1.00	$[C_8C_1im][NTf_2]$
	Ar	1.00	all ILs
$[C_1C_1im]^+$	$[NTf_2]^-$	0.57	$[(SiC)C_1im]$, $[(SiCSiC)C_1im]$, $[(SiOSiC)C_1im]$ $[NTf_2]$
	$[N(CN)_2]^-$	0.66	$[(SiCSiC)C_1im]$, $[(Me_4C_3)C_1im]$, $[(SiOSiC)C_1im]$ $[N(CN)_2]$
	$[B(CN)_4]^-$	0.62	$[(SiCSiC)C_1im]$ $[B(CN)_4]$
	TMS	0.66	$[(SiC)C_1im]$, $[(SiCSiC)C_1im]$ $[Ani]$
	Np	0.68	$[(Np)C_1im]$ $[NTf_2]$; $[(Me_4C_3)C_1im]$ $[Ani]$
$[C_2C_1im]^+$	$(SiC)_2O$	0.68	$[(SiOSiC)C_1im]$ $[Ani]$
	$[NTf_2]^-$	0.55	$[C_8C_1im]$ $[NTf_2]$
TMS	C_4H_{10}	0.78	$[C_8C_1im]$ $[NTf_2]$
	$[NTf_2]^-$	0.66	$[(SiC)C_1im]$, $[(SiCSiC)C_1im]$ $[NTf_2]$
	$[N(CN)_2]^-$	0.49	$[(SiCSiC)C_1im]$ $[NTf_2]$
	$[B(CN)_4]^-$	0.69	$[(SiCSiC)C_1im]$ $[NTf_2]$
	OTf	0.51	$[(SiCSiC)C_1im]$ $[OTf]$
Np	$[NTf_2]^-$	0.68	$[(Np)C_1im]$, $[(Me_4C_3)C_1im]$ $[NTf_2]$
C_4H_{10}	NTf_2^-	0.69	$[C_8C_1im]$ $[NTf_2]$
$(SiC)_2O$	$[NTf_2]^-$	0.64	$[(SiOSiC)C_1im]$ $[NTf_2]$
	$[N(CN)_2]^-$	0.63	$[(SiOSiC)C_1im]$ $[N(CN)_2]$
TMS	TMS	1.00	$[(SiC)C_1im]$ $[NTf_2]$; $[(SiCSiC)C_1im]$ $[Ani]$
Np	Np	1.00	$[(Np)C_1im]$ $[NTf_2]$; $[(Me_4C_3)C_1im]$ $[Ani]$
$(SiC)_2O$	$(SiC)_2O$	1.00	$[(SiOSiC)C_1im]$ $[Ani]$

Simulation boxes that contained 300 ion pairs were used for validation of the force field and for study of the local structure around cavities. Systems composed of 8 Ar atoms plus 100 ion pairs were set up to study the solvation environments around argon. 8 atoms, which allow for reasonable statistics, were placed at the vertices of a cube with an edge length of 20 Å in the middle of the box (which has $L > 40$ Å) and tethered by a harmonic potential of 5 kcal mol⁻¹ to prevent Ar...Ar interactions. These systems were equilibrated for 2 ns, and then 10 or 20 ns trajectories were generated for the pure ILs and the systems with Ar, respectively.

The viscosities of ionic liquid were evaluated from 10 ns non-equilibrium MD trajectories using the periodic perturbation method²³ with applied acceleration of $0.02 \cdot 10^{-5}$ Å fs⁻².⁷ The force field was validated through the comparison of predicted and experimental values of density and viscosity of pure ILs (Table S3). The TRAVIS software²⁴⁻²⁶ was used to compute radial distribution functions around Ar atoms in solution; to evaluate the distributions of void spheres as a function of their radii in the

pure ILs; and to determine which atomic sites are exposed to cavities. Voids with a radius of 1.9Å were chosen for the distribution analysis.

Table S3. Calculated densities and viscosities of pure ILs at 353 K

System	$\rho_{\text{exp}} / \text{g cm}^{-3}$	$\rho_{\text{calc}} / \text{g cm}^{-3}$	$\rho_{\text{dev}} / \%$	$\eta_{\text{exp}} / \text{mPa s}$	$\eta_{\text{calc}} / \text{mPa s}$
[(Np)C ₁ im][NTf ₂]	1.3604	1.3492	-0.82	16.6	8.5 ± 0.2
[(SiC)C ₁ im][NTf ₂]	1.3393	1.3314	-0.59	11.7	7.1 ± 0.1
[C ₈ C ₁ im][NTf ₂]	1.2729	1.2577	-1.20	13.4	8.6 ± 0.2
[(Me ₄ C ₅)C ₁ im][NTf ₂]	1.2778	1.2689	-0.69	38.0	13.5 ± 0.3
[(SiOSiC)C ₁ im][NTf ₂]	1.2580	1.2590	0.08	12.2	6.4 ± 0.1
[(SiOSiC)C ₁ im][DCA]	0.9978	1.0224	2.47	10.4	12.0 ± 0.3
[(SiCSiC)C ₁ im][NTf ₂]	1.2520	1.2315	-1.64	16.1	7.9 ± 0.1
[(SiCSiC)C ₁ im][DCA]	0.9804	0.9830	0.27	16.2	13.6 ± 0.5
[(SiCSiC)C ₁ im][TCB]	0.9460	0.9616	1.65	12.7	25.5 ± 0.8
[(SiCSiC)C ₁ im][OTf]	1.1301	1.1235	-0.58	31.6	16.7 ± 0.5

The chemical potential of Ar in the ionic liquids was calculated using the free energy perturbation (FEP) method, which was enabled in LAMMPS via FEP package. The system was composed of one freely moving Ar atom surrounded by 100 ion pairs of [(SiC)C₁im][NTf₂] or [(SiCSiC)C₁im][NTf₂]. The solute interactions were progressively activated in a simulation box containing the IL: first, the van der Waals interaction with the solvent and then, the electrostatic interaction of the induced dipole with the IL. A coupling parameter, λ , was progressively increased from zero (argon present in the box but not experiencing solute-solvent interactions) to one (argon fully interacting with the solvent), successively for the Lennard-Jones and Coulomb potentials with $d\lambda$ steps of 0.05 and 0.10 respectively. At each value the box was equilibrated for 2 ns, followed by a 2 ns FEP calculation of “creation” ($\lambda+d\lambda$) and “annihilation” ($\lambda-d\lambda$) of the solute molecule, to confirm that hysteresis is negligible. Soft-cores potentials²⁷ were used to avoid singularities at $\lambda = 0$ and 1. An example of a FEP curve is depicted in Figure S2. The chemical potential difference between the initial and the final states was calculated through the relation

$$\Delta\mu = -kT \sum_{i=0}^{i-1} \ln \frac{\langle V \exp(-(U_{\lambda_{i+1}} - U_{\lambda_i})/(kT)) \rangle_{\lambda_i}}{\langle V \rangle_{\lambda_i}} \quad (\text{eq. S1})$$

The free energy of transfer of argon from an ideal gas state to a dilute solution, at constant temperature and pressure, was computed through a thermodynamic cycle (Figure S3). Because Ar has no intramolecular modes, the residual chemical potential corresponds directly to the creation of Ar in an IL. The mole fraction solubility was calculated from

$$x = \frac{p^*}{\rho_{\text{IL}} RT} \exp\left(-\frac{\mu_{\text{res}}}{RT}\right) \quad (\text{eq. S2})$$

where $\rho(\text{IL})$ is the molar density of the IL solvent and p^* is the partial pressure of the gas (1 bar).

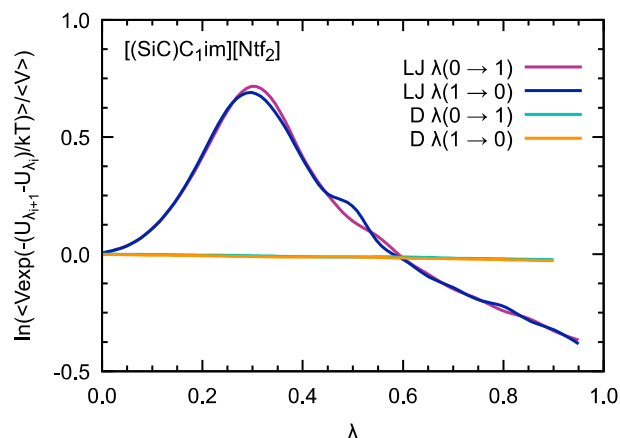


Figure S2. FEP calculation as a function of the activation parameter λ for argon in $[(\text{SiC})\text{C}_1\text{im}][\text{NTf}_2]$. LJ corresponds to the activation of Lennard-Jones potential, D to Drude induced dipole.

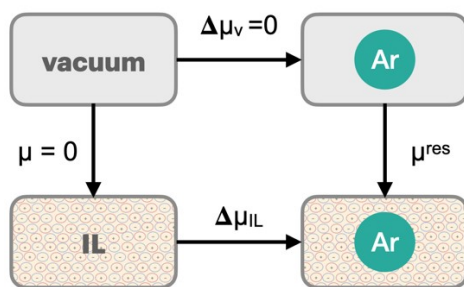


Figure S3. Thermodynamic cycle used to calculate the residual chemical potential.

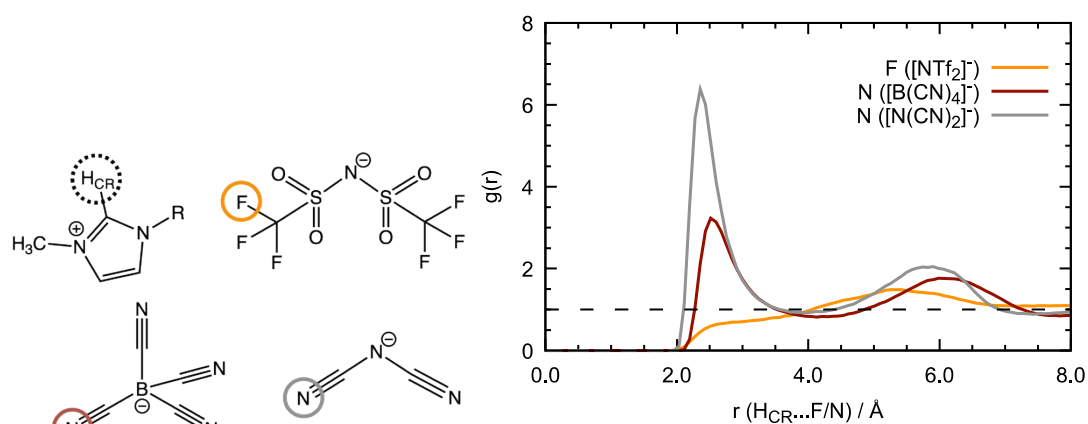


Figure S4. Radial distribution function of atoms of anions around H_{CR} atom of imidazolium ring of $[(\text{SiCSiC})\text{C}_1\text{im}]^+$ in Ar plus $[(\text{SiCSiC})\text{C}_1\text{im}][\text{NTf}_2]$, $[(\text{SiCSiC})\text{C}_1\text{im}][\text{B}(\text{CN})_4]$, or $[(\text{SiCSiC})\text{C}_1\text{im}][\text{N}(\text{CN})_2]$.

4. Analytical methods for structure determination

NMR spectroscopy. ^1H and ^{13}C NMR spectra were recorded on Bruker Fourier 300 MHz spectrometer, chemical shifts were referenced against to the residual NMR solvent signal.²⁸ ^{11}B NMR spectra were recorded on *Bruker Avance* 400 MHz spectrometer.

UHPLC–TOF–HRMS system. Analyses were carried out using an *Agilent* 1290 *Infinity series* LC system coupled to *Agilent* 6230A Accurate-Mass TOF LC/MS with electrospray ionisation (ESI). The UHPLC was equipped with a binary pump (G4220A), an autosampler thermostat (G1330B), an autosampler (G4226A) and a thermostatted column compartment (G1316C). Chromatographic separation was performed at 30 °C using *Agilent Zorbax RRHD Eclipse Plus* C18, 2.1×50 mm, 1.8 μm column. No additional chromatographic separation bands, monitored by the total ion current (TIC), were detected for any of samples analysed under these conditions.

Samples were dissolved in deionised water, filtered through a nylon membrane filter (pore size 0.45 μm) and 1.0 μL of the solution (0.2 mg/mL) was injected into the UHPLC system. The analysis was carried out using 0.1% formic acid in water (A) and acetonitrile (B) as the mobile phase with a flow rate of 0.3 mL min⁻¹. A gradient elution was used according to the following program: 0 min, 5 % B; 7.0 min, 95% B; 10.0 min, 95% B. High resolution mass spectra (HRMS) were taken on an *Agilent* 6230A TOF LC/MS. The mass spectrometry operating conditions in positive and negative ionisation mode were as follows: gas temperature 300 °C, gas flow rate 12 L/min, nebulizer pressure 45 psi, sheath gas temperature 300 °C, sheath gas flow 12 L/min, capillary voltage 4000 V and applied fragmentor 130 V. The full scan mass range was set to 50–500 m/z. External calibration of mass spectrometer for accurate mass measurements was performed according to the manufacturer's guidelines by using ESI-L Low Concentration Tuning Mix (*Agilent Technologies*). Spectrum extraction and peak detection were performed with *MassHunter* 7.00 software (*Agilent*).

5. Synthetic procedures

Potassium tetracyanoborate was prepared as described previously.²⁹

^{11}B NMR (128 MHz, D₂O, δ): -38.5 ppm

1-Octyl-3-methylimidazolium bis(trifluoromethanesulfonyl)imide [C₈C₁im][NTf₂] was synthesized *via* the corresponding Br⁻ salt as described previously.³⁰

^1H NMR (300 MHz, DMSO, δ): 9.11–9.07 (m, 1H), 7.75–7.71 (m, 1H), 7.68–7.64 (m, 1H), 4.15 (t, $^3J_{\text{HH}} = 7.2$ Hz, 2H), 3.85 (s, 3H), 1.87–1.71 (m, 2H), 1.37–1.16 (m, 10H), 0.91–0.79 (m, 3H) ppm

^{13}C NMR (75 MHz, DMSO, δ): 136.9, 124.0, 122.7, 120.0 (q, 2C, $J_{\text{CF}} = 322$ Hz), 49.3, 36.1, 31.6, 29.8, 28.9, 28.8, 25.9, 22.5, 14.2 ppm

Neopentyl mesylate was obtained as described before³¹ and used without further purification.

^1H NMR (300 MHz, CDCl₃, δ): 0.97 (s, 9H), 2.99 (s, 3H), 3.86 (s, 2H) ppm

1-Neopentylimidazole. Sodium imidazolide³² (70.74 g, 786 mmol, 1.4 eq) was dried (100 °C, 0.1 mbar, 1 h) and then dissolved in dry DMSO (250 mL) with heating and stirring. To this solution, at ambient temperature, neopentyl mesylate (91.53 g, 551 mmol, 1.0 eq) was added dropwise with stirring over 30 min. The mixture was heated

(115 °C) and vigorously stirred for 18 h. After cooling, the solids were removed *via* vacuum-filtration using a glass fibre membrane. The clear filtrate was diluted with water (100 mL) and extracted with EtOAc (350 mL). The aqueous layer was further extracted with EtOAc (4 x 50 mL) and all EtOAc phases combined. Further extractions with water (3x50 mL), 5% aqueous LiCl (50 mL) and brine (2 x 50 mL) were performed. The solution was dried over anhydrous MgSO₄. EtOAc was removed *in vacuo* and the crude product distilled under reduced pressure to provide a colourless liquid with a characteristic sweet odour (bp 122-123 °C at 7 Torr, 54.72 g, 72%).

¹H NMR (300 MHz, CDCl₃, δ): 7.40–7.33 (m, 1H), 7.01–6.95 (m, 1H), 6.85–6.79 (m, 1H), 3.65 (s, 2H), 0.91 (s, 9H) ppm

¹³C NMR (75 MHz, CDCl₃, δ): 138.2, 128.6, 120.6, 59.0, 32.6, 27.4 ppm

1-Neopentyl-3-methylimidazolium tosylate [(Np)C₁im][TsO]. 1-Neopentylimidazole (48.31 g, 350 mmol, 1.0 eq) was dissolved in EtOAc (200 mL). To this solution, methyl tosylate (71.92 g, 386 mmol) in EtOAc (100 mL) was added dropwise with stirring over 30 min. White crystals started to form, and the mixture was stirred at 50 °C for 18 h. The suspension was allowed to cool to ambient temperature and then cooled to -20 °C. The product was collected on a Buchner funnel, washed with EtOAc, dried in air and at reduced pressure (50 °C, 0.1 Torr) to afford snow-white flakes (m.p. 121-124 °C, 111.37 g, 98%).

¹H NMR (300 MHz, DMSO-*d*₆, δ): 9.17–9.09 (m, 1H), 7.76–7.66 (m, 2H), 7.55–7.46 (m, 2H), 7.15–7.07 (m, 2H), 3.99 (s, 2H), 3.86 (s, 3H), 2.28 (s, 3H), 0.89 (s, 9H) ppm

¹³C NMR (75 MHz, DMSO-*d*₆, δ): 145.6, 137.7, 137.2, 128.1, 125.5, 123.8, 123.1, 59.4, 35.8, 31.9, 26.6, 20.8 ppm

HRMS (ESI+) m/z: [M]⁺ Calcd for C₉H₁₇N₂⁺ 153.1392; Found 153.1392

HRMS (ESI-) m/z: [M]⁻ Calcd for C₇H₇O₃⁻ 171.0116; Found 171.0120

1-Neopentyl-3-methylimidazolium bis(trifluoromethanesulfonyl)imide [(Np)C₁im][NTf₂]. 1-Neopentyl-3-methylimidazolium tosylate (40.99 g, 126 mmol) was dissolved in water (100 mL) and combined with a solution of LiNTf₂ (36.27 g, 126 mmol) in water (50 mL). DCM was added (50 mL) and the emulsion was vigorously stirred overnight. The organic phase was separated, diluted with DCM (100 mL) and washed with water (5 x 50 mL) in a separatory funnel. The solution was filtered through the hydrophobic filter paper, evaporated *in vacuo* and stirred at reduced pressure (0.1 mbar, 6 h) to afford a colourless viscous liquid (49.81 g, 91%).

¹H NMR (300 MHz, DMSO-*d*₆, δ): 9.09–9.02 (m, 1H), 7.74–7.63 (m, 2H), 3.99 (s, 2H), 3.87 (s, 3H), 0.91 (s, 9H) ppm

¹³C NMR (75 MHz, DMSO-*d*₆, δ): 137.6, 124.2, 123.6, 119.9 (q, 2C, ¹J_{CF} = 321 Hz), 60.0, 36.3, 32.3, 27.0 ppm

HRMS (ESI+) m/z: [M]⁺ Calcd for C₉H₁₇N₂⁺ 153.1392; Found 153.1391

HRMS (ESI-) m/z: [M]⁻ Calcd for C₂F₆NO₄S₂⁻ 279.9173; Found 279.9181

2-chloro-2,4,4-trimethylpentane

2,4,4-Trimethylpent-1-ene (100 g, 0.89 mol) was dissolved in dry diethyl ether (150 mL) and a strong stream of dry hydrogen chloride was passed through the solution until it was saturated, and additionally for 1 hr. The solution was left to stand overnight, extracted with water (100 mL) and a saturated solution of NaHCO₃ (100 mL), and dried over anhydrous MgSO₄. The solvent was removed *in vacuo* and the residue distilled

under reduced pressure to yield 2-chloro-2,4,4-trimethylpentane as a colourless liquid (bp 62-68 °C at 60 Torr, 111,14 g, 84%).

¹H NMR (300 MHz, CDCl₃, δ): 1.88 (s, 2H), 1.67 (s, 6H), 1.05 (s, 9H) ppm. In agreement with previous data.³³

2,2,4,4-tetramethylpentanoic acid³⁴

Bromoethane (14.59 mL, 0.20 mol) was dissolved in anhydrous diethyl ether (95 mL) and added dropwise with vigorous stirring to magnesium turnings (27.30 g, 1.12 mol) under argon. 2-Chloro-2,4,4-trimethylpentane (92.62 g, 0.63 mol) and bromoethane (19.98 mL, 0.27 mol) were dissolved in anhydrous diethyl ether (400 mL) and added to the solution drop by drop. When the reaction subsided, the solution was cooled on ice and a strong stream of dry carbon dioxide was passed through the solution until it separated into two distinct layers, and additionally for 1 hr. The solution was acidified with 10% hydrochloric acid and extracted with petroleum ether (3x100 mL). The organic layer was washed twice with water (100 mL) and extracted with 1 M KOH (630 mL). The alkaline solution was acidified with 10% HCl. 2,2,4,4-Tetramethylpentanoic acid separated as an oil that crystallized on standing overnight (19.04 g, 21%).

¹H NMR (300 MHz, CDCl₃, δ): 11.97 (bs, 1H), 1.66 (s, 2H), 1.24 (s, 6H), 0.95 (s, 9H) ppm. In agreement with previous data.³⁵

2,2,4,4-tetramethylpentan-1-ol³⁶

2,2,4,4-Tetramethylpentanoic acid (19.04 g, 0.13 mol) was dissolved in anhydrous THF (60 mL) and 1 M borane in THF (160 mL, 0.16 mol) was added under argon drop by drop. The solution was refluxed for 2 h and cooled. Water (120 mL) was added followed by 4 M HCl (15 mL) and the solution was stirred overnight. The solution was extracted with petroleum ether, the organic layer was washed twice with water (70 mL) and dried over anhydrous MgSO₄. The solvent was removed, and the residue distilled under reduced pressure to yield 2,2,4,4-tetramethylpentan-1-ol as a colourless liquid (b.p. 90-94 °C at 23 Torr, 13.11 g, 70%).

¹H NMR (300 MHz, CDCl₃, δ): 3.26 (s, 2H), 1.25 (s, 2H), 1.00 – 0.90 (m, 15H) ppm. In agreement with previous data.³⁶

(2,2,4,4-tetramethylpent)-1-yl methanesulfonate

2,2,4,4-tetramethylpentan-1-ol (13.11 g, 0.091 mol) was dissolved in anhydrous DCM (180 mL) and trimethylamine (10.12 g, 0.10 mol) was added to the solution under argon atmosphere. After cooling the resulting mixture in ice/water bath, followed a dropwise addition of methanesulfonyl chloride (11.46 g, 0.10 mol) and the reaction mixture was left stirring. After 2.5 h, water (150 mL) was added and phases were separated. The water phase was extracted with ethyl acetate (3x150 mL) and all the organic layers were combined, washed with water (2x150 mL) and brine (150 mL) and dried over anhydrous MgSO₄. The solvents were removed in *vacuo* and the residue distilled under reduced pressure to yield (2,2,4,4-tetramethylpent)-1-yl methanesulfonate as a colourless liquid (bp 108-112 °C at 0.1 Torr, 16.59 g, 82%).

¹H NMR (300 MHz, DMSO-*d*₆, δ): 3.89 (s, 2H), 2.97 (s, 3H), 1.31 (s, 2H), 1.03 (s, 6H), 0.97 (s, 9H) ppm

3-(2,2,4,4-tetramethylpent)-1-yl-1H-imidazole

(2,2,4,4-tetramethylpent)-1-yl methanesulfonate (16.59 g, 0.074 mol) was dissolved in dry DMSO (50 mL) and sodium imidazolidate³² (7.38 g, 0.082 mol) was added before

flushing the reaction flask with argon. The mixture was heated (115 °C) and stirred for 16 h. The flask was cooled and water (50 mL) was added to it. An extraction with ethyl acetate (3x100 mL) followed. The organic phases were combined and washed with water (3x50 mL) and brine (50 mL). The solution was dried over anhydrous MgSO₄. The solvent was removed in *vacuo* and the crude product was distilled under reduced pressure to yield 3-(2,2,4,4-tetramethylpent)-1-yl-1H-imidazole as a colorless liquid (bp 80-84 °C at 0.1 Torr, 12.65 g, 88%).

¹H NMR (300 MHz, DMSO-*d*₆, δ): 7.36 (d, 1H), 6.98 (t, 1H), 6.82 (t, 1H), 3.67 (s, 2H), 1.25 (s, 2H), 0.97 (d, 15H) ppm

1-Methyl-3-(2,2,4,4-tetramethylpent)-1-yl-1H-imidazol-3-ium tosylate [(Me₄C₅)C₁im][OTs]. 3-(2,2,4,4-Tetramethylpent)-1-yl-1H-imidazole (12.65 g, 0.065 mol) was dissolved in ethyl acetate (50 mL) and methyl tosylate (12.71 g, 0.068 mol) was added. The mixture was left to stand overnight before filtrating it. The filtrated product was washed with a small amount of dry diethyl ether yielding 1-methyl-3-(2,2,4,4-tetramethylpent)-1-yl-1H-imidazol-3-ium tosylate (23.00 g, 93%) as a white solid.

¹H NMR (300 MHz, CDCl₃, δ): 9.07 (d, 1H), 7.70 (dt, 2H), 7.54 – 7.38 (m, 2H), 7.16 – 7.04 (m, 2H), 4.03 (s, 2H), 3.87 (s, 3H), 2.29 (s, 3H), 1.00 (s, 9H), 0.96 (s, 6H) ppm

¹³C NMR (75 MHz, CDCl₃, δ): 143.6, 139.6, 139.1, 128.8, 126.1, 123.6, 123.2, 62.3, 52.6, 36.6, 32.3, 32.0, 26.0, 21.4 ppm (1 C could not be observed at 75 MHz)

HRMS (ESI+) *m/z*: [M]⁺ Calcd for C₁₃H₂₅N₂⁺ 209.2018; Found 209.2021

HRMS (ESI-) *m/z*: [M]⁻ Calcd for C₇H₇O₃S⁻ 171.0116; Found 171.0126

1-Methyl-3-(2,2,4,4-tetramethylpent)-1-yl-1H-imidazol-3-ium bistriflimide [(Me₄C₅)C₁im][NTf₂]. 1-Methyl-3-(2,2,4,4-tetramethylpent)-1-yl-1H-imidazol-3-ium tosylate (23.00 g, 0.060 mol) was dissolved in water (30 mL) and lithium bistriflimide (18.95 g, 0.066 mol) was dissolved in water (30 mL) separately. Both solutions were combined and the resulting mixture was extracted with DCM (3x50 mL). The combined DCM layers were washed with water (10x15 mL) and filtrated through hydrophobic filter paper. DCM was removed in *vacuo* yielding the product: 1-methyl-3-(2,2,4,4-tetramethylpent)-1-yl-1H-imidazol-3-ium bistriflimide (29.50 g, 95 %).

¹H NMR (300 MHz, CD₃OD, δ): 8.88–8.83 (m, 1H), 7.58-7.51 (m, 2H), 4.07 (s, 2H), 3.96-3.92 (m, 3H), 1.39 (s, 2H), 1.07-1.05 (m, 15H) ppm

¹³C NMR (75 MHz, CD₃OD, δ): 138.6, 125.5, 124.3, 121.2 (q, ¹J_{CF} = 322 Hz), 63.0, 53.8, 37.4, 36.5, 33.0, 32.4, 26.4 ppm

HRMS (ESI+) *m/z*: [M]⁺ Calcd for C₁₃H₂₅N₂⁺ 209.2018; Found 209.2023

HRMS (ESI-) *m/z*: [M]⁻ Calcd for C₂F₆NO₄S₂⁻ 279.9173; Found 279.9172

1-(trimethylsilylmethyl)imidazole. Sodium imidazolide³² (45.75 g, 508 mmol, 1.1 eq) was dried (100 °C, 0.1 mbar, 1 h) and then dissolved in dry DMSO (220 mL) with heating and stirring. To this solution, at ambient temperature, chloromethyltrimethylsilane (56.65 g, 462 mmol, 1.0 eq) was added dropwise with stirring over 2 h min. The mixture was stirred at ambient temperature for 14 h and diluted with EtOAc (400 mL). The solids were filtered off and the filtrate diluted with water (450 mL). The aqueous phase was extracted with more EtOAc (3x100 mL). The combined organic phases were washed with water (100 mL), brine (100 mL), dried over anhydrous MgSO₄ and the solvent removed in *vacuo*. The crude product was distilled at reduced pressure provide a colourless liquid (bp 76 °C at 0.1 mbar, 59.93 g, 84%).

¹H NMR (300 MHz, CDCl₃, δ): 7.33 – 7.28 (m, 1H), 7.02 – 6.95 (m, 1H), 6.79 – 6.72 (m, 1H), 3.48 (s, 2H), 0.05 (s, 9H) ppm

^{13}C NMR (75 MHz, CDCl_3 , δ): 137.3, 129.0, 119.8, 38.7, -2.7 ppm

1-(Trimethylsilylmethyl)imidazolium iodide [(SiC) C_1im]I. Iodomethane (0.63 g, 4.4 mmol) was added to a solution of 1-(trimethylsilylmethyl)imidazole (0.57 g, 3.7 mmol) in EtOAc (5 mL). Yellow oil had formed after stirring for 15 h. Acetone (2 mL) was added, and the clear mixture gradually cooled to $-78\text{ }^\circ\text{C}$ with stirring under argon. White crystals were canula-filtered at $-78\text{ }^\circ\text{C}$, washed with Et_2O (4x5 mL) and dried at ambient temperature (0.1 mbar, 4 h).

The dried crystalline 1-methyl-3-(trimethylsilylmethyl)imidazolium iodide (0.50 g) was suspended in EtOAc (400 mL) and iodomethane added (50.46 g, 356 mmol). 1-(trimethylsilylmethyl)imidazole (45.71 g, 296 mmol) was added dropwise to the stirred suspension at ambient temperature over the course of 3 h, affording a suspension of white crystals. The mixture was stirred for further 11 h in dark. The product was collected on a Buchner funnel, washed with ether (4x100 mL) and dried (0.1 mbar, 24 h) to provide white crystals (m.p. $84\text{--}86\text{ }^\circ\text{C}$, 71.53 g, 81%)

^1H NMR (300 MHz, $\text{DMSO-}d_6$, δ): 9.05 – 8.89 (m, 1H), 7.75 – 7.68 (m, 1H), 7.65 – 7.59 (m, 1H), 3.92 (s, 2H), 3.86 (s, 3H), 0.07 (s, 9H) ppm

^{13}C NMR (75 MHz, $\text{DMSO-}d_6$, δ): 135.5, 123.5 (2C), 123.0, 35.8, -3.2 ppm

HRMS (ESI+) m/z: $[\text{M}]^+$ Calcd for $\text{C}_8\text{H}_{17}\text{N}_2\text{Si}^+$ 169.1161; Found 169.1164

HRMS (ESI-) m/z: $[\text{M}]^-$ Calcd for I^- 126.9045; Found 126.9047

1-(Trimethylsilylmethyl)imidazolium bis(trifluoromethanesulfonyl)imide [(SiC) C_1im][NTf $_2$]. 1-(Trimethylsilylmethyl)imidazolium iodide (15.50 g, 52.3 mmol) was dissolved in water (100 mL), and lithium bis(trifluoromethanesulfonyl)imide (15.02 g, 52.3 mmol) in a minimal amount of water was added. The mixture was

extracted with DCM (4x50 mL). The combined organic phases were first washed with water (50 mL) and a few drops of 2% $\text{Na}_2\text{S}_2\text{O}_3$ solution, and then with more water (6x20 mL) until the washings tested negative with 0.1M AgNO_3 solution. The DCM phase was filtered through the hydrophobic filter paper. The solvent was evaporated in *vacuo* and the remainder stirred at reduced pressure ($60\text{ }^\circ\text{C}$, 0.1 mbar, 12 h) to afford a colourless liquid (19.34 g, 82%).

^1H NMR (300 MHz, $\text{DMSO-}d_6$, δ): 8.94 – 8.88 (m, 1H), 7.68 – 7.62 (m, 1H), 7.57 – 7.51 (m, 1H), 3.88 (s, 2H), 3.85 (s, 3H), 0.08 (s, 9H) ppm

^{13}C NMR (75 MHz, $\text{DMSO-}d_6$, δ): 135.7, 123.6, 123.0, 119.5 (q, 2C, $^1J_{\text{CF}} = 322\text{ Hz}$), 40.7, 35.7, -3.4 ppm

HRMS (ESI+) m/z: $[\text{M}]^+$ Calcd for $\text{C}_8\text{H}_{17}\text{N}_2\text{Si}^+$ 169.1161; Found 169.1164

HRMS (ESI-) m/z: $[\text{M}]^-$ Calcd for I^- 126.9045; Found 126.9047

1-Chloro-2,2,4,4-tetramethyl-2,4-disilapentane was prepared according to a literature procedure.³⁷ Colourless oil was obtained (11.59 g, 81%).

^1H NMR (300 MHz, CDCl_3 , δ): -0.14 (s, 2H) 0.05 (s, 9H), 0.14 (s, 6H), 2.75 (s, 2H) ppm

^{13}C NMR (75 MHz, CDCl_3 , δ): -1.9, 1.3, 1.4, 32.5 ppm

1-(2,2,4,4-tetramethyl-2,4-disilapentyl)-3-methylimidazolium chloride [(SiCSiC) C_1im]Cl. 1-Chloro-2,2,4,4-tetramethyl-2,4-disilapentane (46.93 g, 241 mmol, 1.3 eq) was added to a solution of 1-methylimidazole (15.21 g, 185 mmol, 1.0 eq) in dry acetonitrile (100 mL) with stirring. The solution was stirred for 3 weeks

at $60\text{ }^\circ\text{C}$. No residual 1-methylimidazole could be detected (NMR) in the reaction mixture after this time. The reaction mixture was cooled down to ambient temperature,

roughly half of the solvent was evaporated *via* rotary evaporation and remaining mixture was cooled down to 0 °C. Crystallization from acetonitrile with dropwise addition of ethyl acetate (anti-solvent) using a seed crystal was done. The crystallization was allowed to complete at -20 °C, vacuum filtered and dried at reduced pressure (0.1 mbar, 50 °C, 8 h). White crystals were obtained (mp. 69-71 °C, 37.80 g, 74%).

¹H NMR (300 MHz, DMSO, δ): 9.07 – 8.97 (m, 1H), 7.77 – 7.66 (m, 1H), 7.64 – 7.56 (m, 1H), 3.92 – 3.75 (m, 5H), 0.08 (s, 6H), 0.03 (s, 9H), -0.15 (s, 2H) ppm

¹³C NMR (75 MHz, DMSO-*d*₆, δ): -1.8, 0.8, 1.8, 31.2, 36.2, 42.1, 123.6, 123.9, 124.0, 136.1 ppm

HRMS (ESI+) *m/z*: [M]⁺ Calcd for C₁₁H₂₅N₂Si₂⁺ 209.2018; Found 209.2023

1-(2,2,4,4-tetramethyl-2,4-disilapentyl)-3-methylimidazolium dicyanamide
[(SiCSiC)₂im][N(CN)₂].

1-(2,2,4,4-tetramethyl-2,4-disilapentyl)-3-methylimidazolium chloride (22.52 g, 81.3 mmol) was dissolved in water (150 mL), powdered charcoal was added and the solution stirred at 60 °C for 1 h. After cooling to 0 °C the suspension was gravity filtered. To this solution sodium dicyanamide (7.24 g, 81.3 mmol) in water (50 mL) was added. The mixture was extracted with dichloromethane (4x60 mL) and the combined organic phases washed with water (9x30 mL). Organic phase was filtered through the hydrophobic filter paper and a 40 μ m PTFE filter, the solvent removed in *vacuo* and the ionic liquid stirred at reduced pressure (60 °C, 0.1 mbar, 4 h) to afford a colourless liquid (19.67 g, 79%).

¹H NMR (300 MHz, DMSO-*d*₆, δ): 8.94 – 8.88 (m, 1H), 7.70 – 7.64 (m, 1H), 7.60 – 7.54 (m, 1H), 3.89 – 3.78 (m, 5H), 0.09 (s, 6H), 0.03 (s, 9H), -0.14 (s, 2H) ppm

¹³C NMR (75 MHz, DMSO-*d*₆, δ): 135.5, 123.5, 123.0, 119.1 ([N(CN)₂]⁻), 41.7, 35.7, 1.2, 0.2, -2.3 ppm

HRMS (ESI+) *m/z*: [M]⁺ Calcd for C₁₁H₂₅N₂Si₂⁺ 241.1556; Found 241.1563

HRMS (ESI-) *m/z*: [M]⁻ Calcd for C₂N₃⁻ 66.0092; Found 66.0092

1-(2,2,4,4-tetramethyl-2,4-disilapentyl)-3-methylimidazolium triflate
[(SiCSiC)₂im][OTf].

1-(2,2,4,4-tetramethyl-2,4-disilapentyl)-3-methylimidazolium chloride (21.39 g, 77.2 mmol) was dissolved in water (200 mL), powdered charcoal was added and the solution stirred at 60 °C for 1 h. After cooling to 0 °C the suspension was gravity filtered and combined with a solution of lithium triflate (12.04 g, 77.2 mmol) in water (50 mL). The mixture was extracted with dichloromethane (4x60 mL) and the combined organic phases washed with water (8x30 mL) until the washings tested negative with 0.1M AgNO₃ solution. Organic phase was filtered through the hydrophobic filter paper, a 40 μ m PTFE filter, the solvent evaporated in *vacuo* and the remaining ionic liquid was stirred at reduced pressure (60 °C, 0.1 mbar, 4 h) to afford a viscous colourless liquid (23.36 g, 78%).

¹H NMR (300 MHz, DMSO-*d*₆, δ): 8.95–8.86 (m, 1H), 7.70–7.64 (m, 1H), 7.60–7.53 (m, 1H), 3.89–3.81 (m, 5H), 0.08 (s, 6H), 0.03 (s, 9H), -0.15 (s, 2H) ppm

¹³C NMR (101 MHz, DMSO-*d*₆, δ): 136.0, 124.0, 123.6, 121.2 (q, ¹J_{CF} = 322 Hz), 42.2, 36.2, 1.7, 0.7, -1.8 ppm

1-(2,2,4,4-tetramethyl-2,4-disilapentyl)-3-methylimidazolium tetracyanoborate
[(SiCSiC)₂im][B(CN)₄].

1-(2,2,4,4-tetramethyl-2,4-disilapentyl)-3-methylimidazolium chloride (9.25 g, 33.4 mmol) was dissolved in water (100 mL), powdered charcoal was added and the solution stirred at 60 °C for 1 h. After cooling to 0 °C the suspension was gravity filtered. Potassium tetracyanoborate (5.14 g, 33.4 mmol) was dissolved in water with heating (60 mL) and treated with charcoal in a similar fashion. The clear solutions of both salts were combined and extracted with

DCM (4x60 mL). The combined organic layers were washed with water (8x30 mL) and filtered through the hydrophobic filter paper and a 40 μm PTFE filter. The solvent was evaporated in *vacuo* and the remaining ionic liquid stirred at reduced pressure (60 $^{\circ}\text{C}$, 0.1 mbar, 4 h) to afford a colourless liquid (10.32 g, 87%).

^1H NMR (300 MHz, $\text{DMSO-}d_6$, δ): 8.96–8.85 (m, 1H), 7.67–7.59 (m, 1H), 7.55–7.47 (m, 1H), 3.90–3.78 (m, 5H), 0.10 (s, 6H), 0.04 (s, 9H), -0.14 (s, 2H) ppm

^{13}C NMR (75 MHz, $\text{DMSO-}d_6$, δ): -2.4, 0.2, 1.2, 35.7, 41.8, 121.8 (q, $^1J_{\text{CB}}=70.8$ Hz), 123.0, 123.5, 135.6 ppm

HRMS (ESI+) m/z : $[\text{M}]^+$ Calcd for $\text{C}_{11}\text{H}_{25}\text{N}_2\text{Si}_2^+$ 241.1556; Found 241.1556

HRMS (ESI-) m/z : $[\text{M}]^-$ Calcd for C_4BN_4^- 115.0217; Found 115.0216

1-(2,2,4,4-tetramethyl-2,4-disilapentyl)-3-methylimidazolium

bis(trifluoromethanesulfonyl)imide [(SiCSiC) $\text{C}_{1\text{im}}$][NTf $_2$]. 1-(2,2,4,4-tetramethyl-2,4-disilapentyl)-3-methylimidazolium chloride (10.31 g, 37.2 mmol) was dissolved in water (100 mL), powdered charcoal was added and the solution stirred at 60 $^{\circ}\text{C}$ for 1 h. After cooling to 0 $^{\circ}\text{C}$ the suspension was gravity-filtered. Lithium bis(trifluoromethanesulfonyl)imide (10.66 g, 37.1 mmol) in a minimal amount of water was combined with the chloride solution, and the mixture extracted with DCM (4x50 mL). The combined organic layers were washed with water (5x20 mL) until the washings tested negative with 0.1M AgNO_3 solution. The DCM phase was filtered through the hydrophobic filter paper and a 40 μm PTFE filter. The solvent was evaporated in *vacuo* and the remaining ionic liquid stirred at reduced pressure (60 $^{\circ}\text{C}$, 0.1 mbar, 10 h) to afford a colourless liquid (17.44 g, 90%).

^1H NMR (300 MHz, $\text{DMSO-}d_6$, δ): 8.94 – 8.88 (m, 1H), 7.69 – 7.69 (m, 1H), 7.58 – 7.58 (m, 1H), 3.84 – 3.83 (m, 5H), 0.08 (s, 6H), 0.03 (s, 9H), -0.15 (s, 2H) ppm

^{13}C NMR (75 MHz, $\text{DMSO-}d_6$, δ): 135.6, 123.5, 123.1, 119.5 (q, 2C, $^1J_{\text{CF}} = 322$ Hz), 41.8, 35.7, 1.2, 0.3, -2.3 ppm

HRMS (ESI+) m/z : $[\text{M}]^+$ Calcd for $\text{C}_{11}\text{H}_{25}\text{N}_2\text{Si}_2^+$ 241.1556; Found 241.1560

HRMS (ESI-) m/z : $[\text{M}]^-$ Calcd for $\text{C}_2\text{F}_6\text{NO}_4\text{S}_2^-$ 279.9173; Found 279.9176

1-Chloro-2,2,4,4,6,6-hexamethyl-2,4,6-trisilaheptane. Grignard reagent was prepared under argon using magnesium shavings (3.98 g, 166 mmol), distilled 1-chloro-2,2,4,4-tetramethyl-2,4-disilapentane (30.23 g, 155 mmol), THF (200 mL), a small crystal of iodine and a few drops of 1,2-dibromoethane. First, iodine was added to the stirred suspension of magnesium in THF. A dropwise addition of the chloroalkane was started, followed by addition of 1,2-dibromoethane. Once the exothermic reaction commenced, the addition of chloroalkane was maintained at a rate that sustained a moderate boiling. After the addition was complete, the mixture was refluxed for 1 h and cooled to ambient temperature. Chloromethyldimethylchlorosilane (20.91 g, 146 mmol) was added dropwise over 10 min to the stirred Grignard reagent. No noticeable heat evolution was observed over the next hour. The reaction mixture was stirred for 1 h at 55 $^{\circ}\text{C}$ and left stirring for 15 h in the warm oil bath without additional heating. The reaction mixture was diluted with water (150 mL). The mixture was extracted with petroleum ether (2x100 mL). Combined organic phases were washed with water (3x50 mL), filtered through the hydrophobic filter paper, dried over anhydrous MgSO_4 and evaporated in *vacuo*. The crude product (45.10 g) was distilled at reduced pressure to provide a colourless liquid (127 $^{\circ}\text{C}$, 7 torr, 29.20 g, 75%).

^1H NMR (300 MHz, CDCl_3 , δ): -0.24 (s, 2H), -0.13 (s, 2H), 0.03 (s, 9H), 0.08 (s, 6H), 0.15 (s, 6H), 2.75 (s, 2H) ppm

^{13}C NMR (75 MHz, CDCl_3 , δ): -1.7, 1.6, 2.5, 2.6, 5.8, 32.6 ppm

1-(2,2,4,4,6,6-hexamethyl-2,4,6-trisilaheptyl)-3-methylimidazolium chloride [(SiCSiCSiC)₃im]Cl. 1-Chloro-2,2,4,4,6,6-hexamethyl-2,4,6-trisilaheptane (19.64 g, 73.5 mmol) was dissolved in EtOAc (20 mL), 1-methylimidazole (19.41 g, 236 mmol) added and the solution stirred at 55 °C until the silane was fully consumed according to NMR (6 days). The volatiles, including excess 1-methylimidazole, were removed in *vacuo* at 70 °C. The remainder was allowed to solidify, twice recrystallized from acetone by cooling to +5 °C, and dried at reduced pressure (50 °C, 0.1 mbar) to provide white flakes (m.p. 69-71 °C, 12.21 g, 48%).

¹H NMR (300 MHz, CDCl₃, δ): 10.14-10.10 (m, 1H), 7.63-7.60 (m, 1H), 7.11-7.08 (m, 1H), 4.04 (s, 3H), 3.84 (s, 2H), 0.10 (s, 6H), -0.01 (s, 6H), -0.07 (s, 9H), -0.25 (s, 2H), -0.33 (s, 2H) ppm

¹³C NMR (75 MHz, CDCl₃, δ): 137.2, 123.7, 122.3, 43.3, 36.6, 5.7, 2.6, 2.3, 1.4, -1.8 ppm

HRMS (ESI+) m/z: [M]⁺ Calcd for C₁₁H₃₃N₂Si₃⁺ 313.1952; Found 313.1947

1-(2,2,4,4,6,6-hexamethyl-2,4,6-disilaheptyl)-3-methylimidazolium

bis(trifluoromethanesulfonyl)imide [(SiCSiCSiC)₂im][NTf₂]. 1-(2,2,4,4,6,6-hexamethyl-2,4,6-trisilaheptyl)-3-methylimidazolium chloride (7.44 g, 21.3 mmol) was dissolved in water (50 mL), and lithium bis(trifluoromethanesulfonyl)imide (6.12 g, 21.3 mmol) in a minimal amount of water was added. The mixture was extracted with DCM (4x50 mL). The combined organic phases were washed with water (5x50 mL) until the washings tested negative with 0.1M AgNO₃ solution. The DCM phase was filtered through the hydrophobic filter paper. The solvent was evaporated in *vacuo* and the remainder stirred at reduced pressure (60 °C, 0.1 mbar, 8 h) to afford a colourless liquid (11.29 g, 89%).

¹H NMR (300 MHz, CDCl₃, δ): 8.61-8.55 (m, 1H), 7.35-7.31 (m, 1H), 7.16-7.11 (m, 1H), 3.91 (s, 3H), 3.75 (s, 2H), 0.13 (s, 6H), 0.06 (s, 6H), 0.00 (s, 9H), -0.22 (s, 2H), -0.26 (s, 2H) ppm

¹³C NMR (75 MHz, CDCl₃, δ): 135.5, 123.9, 123.1, 119.9 (q, 2C, ¹J_{CF} = 322 Hz), 43.4, 36.3, 5.7, 2.34, 2.29, 1.4, -2.1 ppm (1 C not observable at 75 MHz)

HRMS (ESI+) m/z: [M]⁺ Calcd for C₁₁H₃₃N₂Si₃⁺ 313.1952; Found 313.1955

HRMS (ESI-) m/z: [M]⁻ Calcd for C₂F₆NO₄S₂⁻ 279.9173; Found 279.9176

1-(Chloromethyl)-1,1,3,3,3-pentamethyldisiloxane.

Chloro(chloromethyl)dimethylsilane (20.00 g, 0.139 mol) was dissolved in THF, to this solution potassium trimethylsilanolate in THF (71 mL, 0.140 mol) was added dropwise over 30 min with stirring. The mixture was cooled to the room temperature in an ice-water bath. Water (200 mL) and petroleum ether (100 mL) were added to the mixture. After shaking the aqueous phase was separated and further extracted with petroleum ether (3 x 60 mL). The combined organic phases were washed with water (30 mL), dried over Na₂SO₄ and evaporated in *vacuo*. The remaining oil was purified *via* fractional distillation at reduced pressure. Colourless liquid was obtained (9.73 g, 36 %).

¹H NMR (300 MHz, CDCl₃, δ): 2.71 (s, 2H), 0.19 (s, 6H), 0.09 (s, 9H) ppm

¹³C NMR (75 MHz, CDCl₃, δ): 31.1, 2.0, -1.1 ppm

1-Methyl-3-pentamethyldisiloxymethylimidazolium chloride [(SiOSiC)₁im]Cl.

1-(Chloromethyl)-1,1,3,3,3-pentamethyldisiloxane (9.73 g, 49.4 mmol, 1.3 eq.) was added to a stirred solution of 1-methylimidazole (3.30 g, 41.2 mmol, 1.0 eq) in MeCN (45 mL). The solution was stirred at 60 °C until the imidazole was fully consumed according to NMR (2 weeks). The reaction mixture was cooled to 0 °C upon which crystals had formed. The crystallization was completed by dropwise addition of EtOAc while cooling at -20 °C. The product was collected on a Buchner funnel, washed with EtOAc (15 mL) and dried at reduced pressure (50 °C, 0.1 mbar) to provide white crystals (m.p. 141-143 °C, 8.41 g, 73%).

¹H NMR (300 MHz, DMSO-*d*₆, δ): 9.06–8.96 (m, 1H), 7.78–7.67 (m, 1H), 7.61–7.51 (m, 1H), 3.94–3.79 (m, 5H), 0.17 (s, 6H), 0.04 (s, 9H) ppm

¹³C NMR (75 MHz, DMSO-*d*₆, δ): 136.4, 124.1, 123.6, 41.5, 36.2, 2.2, -0.5 ppm

HRMS (ESI+) m/z: [M]⁺ Calcd for C₁₀H₂₃OSi₂⁺ 243.1349; Found 243.1343

1-Methyl-3-pentamethyldisiloxymethylimidazolium dicyanamide [(SiOSiC)₁im][N(CN)₂].

1-Methyl-3-pentamethyldisiloxymethylimidazolium chloride (14.02 g, 50.3 mmol, 1.0 eq.) was dissolved in water (50 mL) and a solution of sodium dicyanamide (4.47 g, 50.3 mmol, 1.0 eq.) in water (50 mL) was added. The mixture was extracted with dichloromethane (5 x 50 mL) and the combined organic phases washed with water. The DCM phase was filtered through the hydrophobic filter paper. The solvent was evaporated in *vacuo* and the remainder stirred at reduced pressure (60 °C, 0.1 mbar, 6 h) to afford a nearly colourless liquid (11.82 g, 76%).

¹H NMR (300 MHz, DMSO-*d*₆, δ): 8.93–8.89 (m, 1H), 7.71–7.67 (m, 1H), 7.55–7.52 (m, 1H), 3.89–3.84 (m, 5H), 0.17 (s, 6H), 0.05 (s, 9H) ppm

¹³C NMR (75 MHz, DMSO-*d*₆, δ): 135.8, 123.6, 123.1, 119.1 ([N(CN)₂]⁻), 41.1, 35.7, 1.7, -1.1 ppm

HRMS (ESI+) m/z: [M]⁺ Calcd for C₁₀H₂₃OSi₂⁺ 243.1349; Found 243.1347

HRMS (ESI-) m/z: [M]⁻ Calcd for C₂N₃⁻ 66.0092; Found 66.0101

1-Methyl-3-pentamethyldisiloxymethylimidazolium tetracyanoborate [(SiOSiC)₁im][B(CN)₄].

Potassium tetracyanoborate (5.00 g, 32.5 mmol, 1.0 eq.) was dissolved in water with heating (60 mL) and the solution treated with charcoal as for [(SiCSiC)₁im][B(CN)₄]. To the aqueous solution of K[B(CN)₄] 1-methyl-3-pentamethyldisiloxymethylimidazolium chloride (9.05 g, 32.45 mol, 1.0 eq.) in water (70 mL) was added. This mixture was extracted with dichloromethane (4 x 50 mL) and the combined organic phases washed with water (6 x 20 mL). Organic phase was filtered through the hydrophobic filter paper and DCM evaporated in *vacuo*. The remainder was stirred at reduced pressure (60 °C, 0.1 mbar, 6 h) to afford a colourless liquid (9.71 g, 84%).

¹H NMR (300 MHz, DMSO-*d*₆, δ): 8.91 (s, 1H), 7.71-7.68 (m, 1H), 7.55-7.51 (m, 1H), 3.88-3.83 (m, 5 H), 0.18 (s, 6H), 0.05 (s, 9H) ppm

¹³C NMR (75 MHz, DMSO-*d*₆, δ): 135.8, 123.6, 123.1, 121.8 (q, ¹J_{CB}=70.8 Hz), 41.1, 35.7, 41.1, 35.7, 1.7, -1.0 ppm

HRMS (ESI+) m/z: [M]⁺ Calcd for C₁₀H₂₃OSi₂⁺ 243.1349; Found 243.1348

HRMS (ESI-) m/z: [M]⁻ Calcd for C₄BN₄⁻ 115.0217; Found 115.0221

1-(Pentamethyldisiloxymethyl)-3-methylimidazolium

bis(trifluoromethanesulfonyl)imide [(SiOSiC)₁im][NTf₂]. 1-Methyl-3-pentamethyldisiloxymethylimidazolium chloride [(SiOSiC)₁im]Cl (7.99 g, 28.7 mmol) was dissolved in water (20 mL), and lithium

bis(trifluoromethanesulfonyl)imide (8.22 g, 28.7 mmol) in a minimal amount of water was added. The mixture was extracted with DCM (2x50 mL). The combined organic phases were washed with water (5 x 20 mL) until the washings tested negative with 0.1M AgNO₃ solution. The DCM phase was filtered through the hydrophobic filter paper. The solvent was evaporated in *vacuo* and the remainder stirred at reduced pressure (60 °C, 0.1 mbar, 4 h) to afford a colourless viscous liquid (14.02 g, 93%).

¹H NMR (300 MHz, DMSO-*d*₆, δ): 8.91 (bs, 1H), 7.71-7.65 (m, 1H), 7.55-7.50 (m, 1H), 3.89-3.83 (m, 5 H), 0.17 (s, 6H), 0.04 (s, 9H) ppm

¹³C NMR (75 MHz, DMSO-*d*₆, δ): 135.8, 123.6, 123.2, 119.5 (q, 2C, ¹J_{CF} = 322 Hz), 41.1, 35.7, 1.6, -1.1 ppm

HRMS (ESI+) m/z: [M]⁺ Calcd for C₁₀H₂₃OSi₂⁺ 243.1349; Found 243.1341

HRMS (ESI-) m/z: [M]⁻ Calcd for C₂F₆NO₄S₂⁻ 279.9173; Found 279.9173

6. High resolution mass spectra

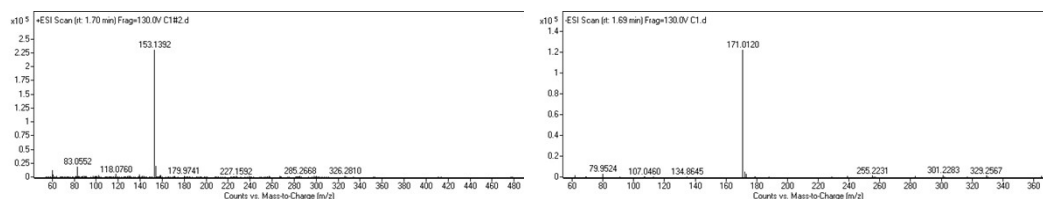


Figure S5. High resolution mass spectra of $[(\text{Np})\text{C}_{1\text{im}}][\text{TsO}]$.

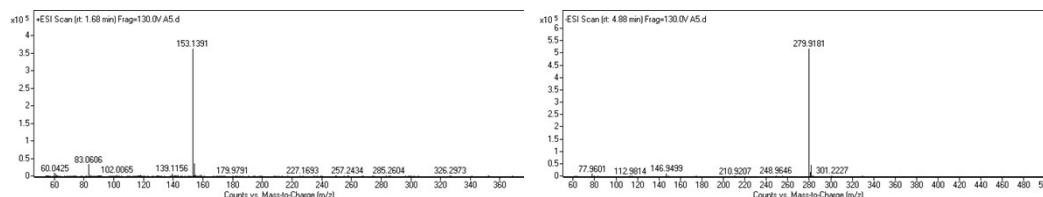


Figure S6. High resolution mass spectra of $[(\text{Np})\text{C}_{1\text{im}}][\text{NTf}_2]$.

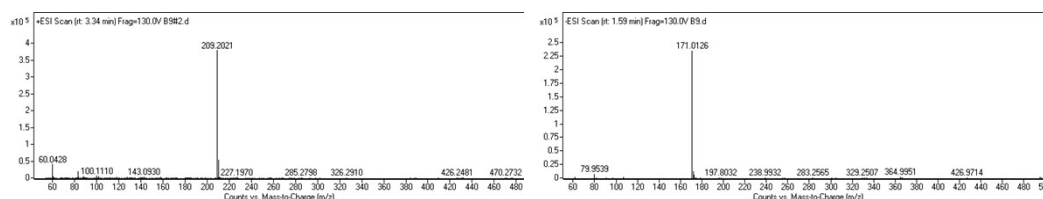


Figure S7. High resolution mass spectra of $[(\text{Me}_4\text{C}_5)\text{C}_{1\text{im}}][\text{TsO}]$.

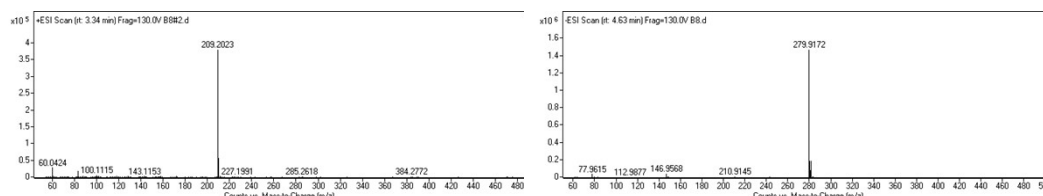


Figure S8. High resolution mass spectra of $[(\text{Me}_4\text{C}_5)\text{C}_{1\text{im}}][\text{NTf}_2]$.

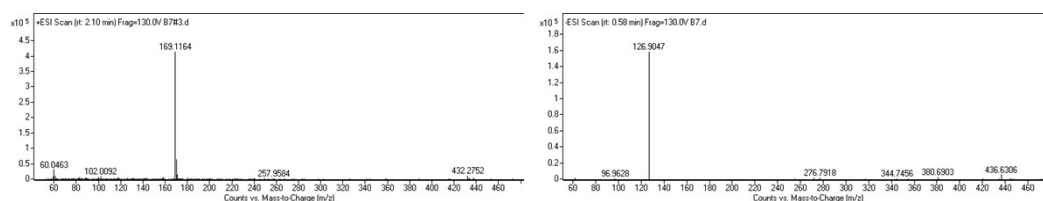


Figure S9. High resolution mass spectra of $[(\text{SiC})\text{C}_{1\text{im}}][\text{TsO}]$.

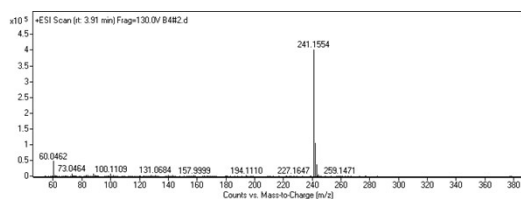


Figure S10. High resolution mass spectra of $[(\text{SiCSiC})\text{C}_1\text{im}]\text{Cl}$.

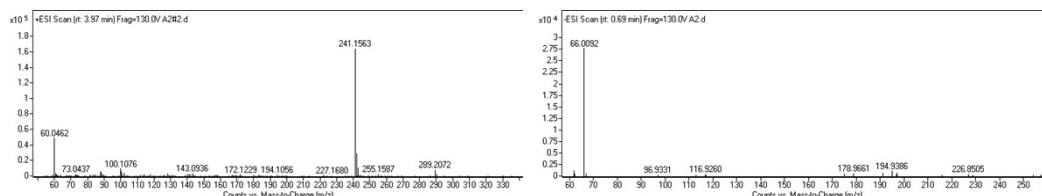


Figure S11. High resolution mass spectra of $[(\text{SiCSiC})\text{C}_1\text{im}][\text{N}(\text{CN})_2]$.

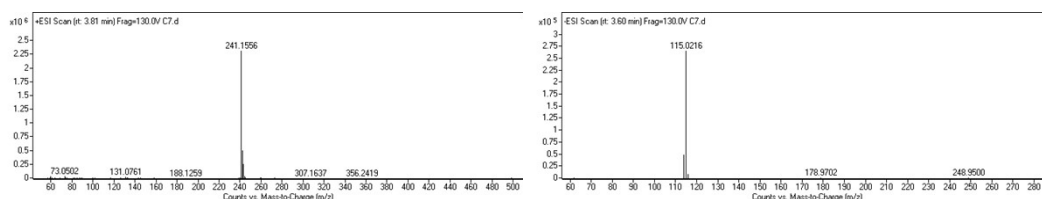


Figure S12. High resolution mass spectra of $[(\text{SiCSiC})\text{C}_1\text{im}][\text{B}(\text{CN})_4]$.

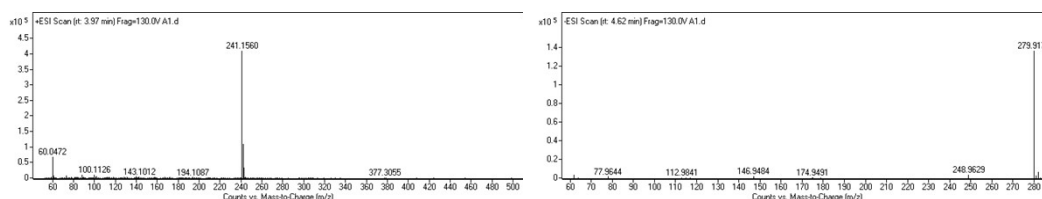


Figure S13. High resolution mass spectra of $[(\text{SiCSiC})\text{C}_1\text{im}][\text{NTf}_2]$.

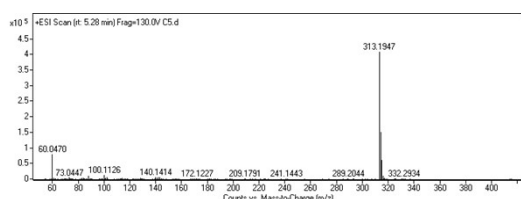


Figure S14. High resolution mass spectra of $[(\text{SiCSiCSiC})\text{C}_1\text{im}]\text{Cl}$.

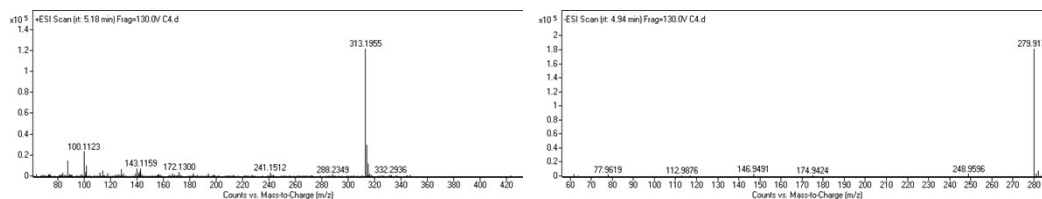


Figure S15. High resolution mass spectra of $[(\text{SiCSiCSiC})\text{C}_1\text{im}][\text{NTf}_2]$.

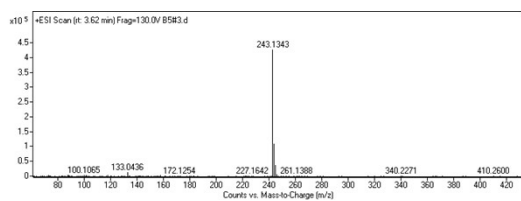


Figure S16. High resolution mass spectra of $[(\text{SiOSiC})\text{C}_1\text{im}]\text{Cl}$.

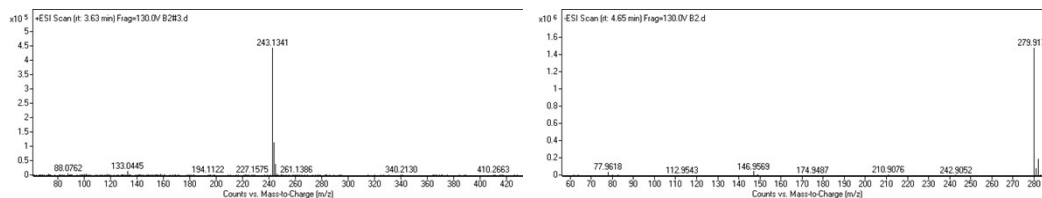


Figure S17. High resolution mass spectra of $[(\text{SiOSiC})\text{C}_1\text{im}][\text{NTf}_2]$.

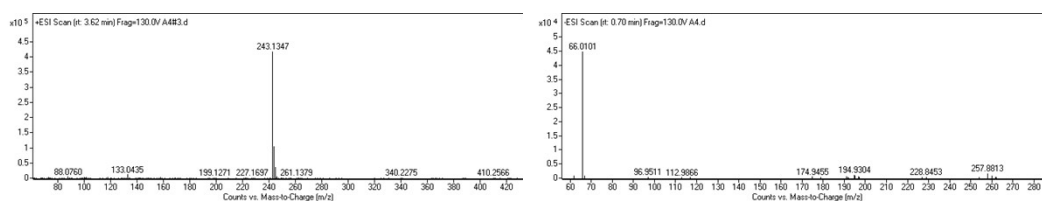


Figure S18. High resolution mass spectra of $[(\text{SiOSiC})\text{C}_1\text{im}][\text{N}(\text{CN})_2]$.

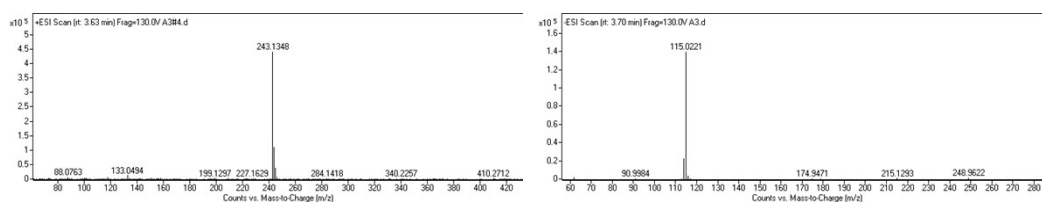


Figure S19. High resolution mass spectra of $[(\text{SiOSiC})\text{C}_1\text{im}][\text{B}(\text{CN})_4]$.

7. Density fitting parameters

Table S4. Summary of the linear fitting parameters for ionic liquid density as a function of temperature, $\rho = a \cdot T + b$. Water content < 233 ppm

No	Ionic Liquid	Temperature range	a , 10^{-4} (g·K ⁻¹ ·cm ⁻³)	b , (g·cm ⁻³)	R^2	w H ₂ O, ppm
1	[(Np)C ₁ im][NTf ₂]	293.15-353.15 K	-9.252661	1.686893	0.99993	34
2	[(SiC)C ₁ im][NTf ₂]	293.15-353.15 K	-9.300606	1.667572	0.99995	70
3	[(SiCSiC)C ₁ im][B(CN) ₄]	293.15-353.15 K	-6.780068	1.185237	0.99992	73
4	[(SiCSiC)C ₁ im][N(CN) ₂]	293.15-353.15 K	-6.040956	1.193665	0.99994	53
5	[(SiCSiC)C ₁ im][OTf]	298.15-353.15 K	-7.371665	1.390292	0.99994	200
6	[(SiCSiC)C ₁ im][NTf ₂]	293.15-353.15 K	-8.680407	1.558452	0.99995	69
7	[(SiO)SiC)C ₁ im][B(CN) ₄]	293.15-353.15 K	-7.217888	1.210442	0.99992	81
8	[(SiO)SiC)C ₁ im][N(CN) ₂]	293.15-353.15 K	-6.594247	1.230478	0.99994	138
9	[(SiO)SiC)C ₁ im][NTf ₂]	293.15-353.15 K	-9.155336	1.581150	0.99995	
10	[(Me ₄ C ₅)C ₁ mim][NTf ₂]	293.15-353.15 K	-8.536809	1.579075	0.99996	24
11	[(SiCSiCSiC)C ₁ im][NTf ₂]	293.15-353.15 K	-8.227302	1.472596	0.9994	47

8. Ionic liquid viscosity fitting parameters

Table S5. Non-linear fitting parameters for Vogel-Fülcher-Tammann-Hesse equation, $\ln \eta = A + B/(T-T_0)$, used for the interpolation of pure ionic liquid viscosity η (mPa·s) as a function of temperature (T). Water content < 233 ppm

No	Ionic Liquid	Temperature range	No of data points	<i>A</i>	<i>B</i> , K	<i>T</i> ₀ , K	ARD, %
1	[(Np)C ₁ im][NTf ₂]	293.15-353.15 K	7	-1.42666	644.666	201.029	0.180
2	[(SiC)C ₁ im][NTf ₂]	293.15-353.15 K	7	-1.45516	637.864	190.126	0.203
3	[(SiCSiC)C ₁ im][B(CN) ₄]	293.15-353.15 K	7	-1.64002	672.639	192.222	0.214
4	[(SiCSiC)C ₁ im][N(CN) ₂]	293.15-353.15 K	7	-1.49051	703.390	188.611	0.178
5	[(SiCSiC)C ₁ im][OTf]	298.15-353.15 K	6	-1.78298	840.159	192.706	0.120
6	[(SiCSiC)C ₁ im][NTf ₂]	293.15-353.15 K	7	-1.48401	694.438	190.070	0.188
7	[(SiO)SiC)C ₁ im][B(CN) ₄]	293.15-333.15 K	6	-1.44057	603.443	184.315	1.700
8	[(SiO)SiC)C ₁ im][N(CN) ₂]	293.15-353.15 K	9	-1.15133	586.361	185.339	0.183
9	[(SiO)SiC)C ₁ im][NTf ₂]	293.15-353.15 K	8	-1.32627	652.229	182.087	0.048
10	[(Me ₄ C ₅)C ₁ mim][NTf ₂]	298.15-353.15 K	7	-2.62425	1005.018	192.346	0.173
11	[(SiCSiCSiC)C ₁ im][NTf ₂]	293.15-353.15 K	8	-1.81919	858.634	176.440	0.057

9. Viscosities of [(SiOSiC)C₁im]⁺ ionic liquids reported in literature

Table S6. Summary of the viscosities of [(SiOSiC)C₁im]⁺ ionic liquids reported in literature, and method used in the measurement

Anion	Temperature	Viscosity, mPa s	Method	Ref.
[NTf ₂] ⁻	298 K	89.0	Reciprocating piston viscometry	38
[NTf ₂] ⁻	293 K	100.8	Stabinger AP SVM3000	39
[NTf ₂] ⁻	298 K	75.59	Rotation viscometer	40
[NTf ₂] ⁻	296 K	87.1	Cone-plate viscometry	41
[C(CN) ₃] ⁻	293 K	60.21	Stabinger AP SVM3000	39
[FSI] ⁻	296 K	76.5	Cone-plate viscometry	41
[BETI] ⁻	296 K	871.5	Cone-plate viscometry	41
[PF ₆] ⁻	296 K	548.6	Cone-plate viscometry	41
[Al(hfip) ₄] ⁻	298 K	34.03	Rotation viscometer	40

10. Gas solubility measurements

To study the solubility of argon in different ionic liquids, multiple experimental data points were obtained in the temperature interval between 303-343 K. Thermodynamic equilibrium is attained when the pressure of the gas above the liquid is stable to within ± 0.05 mbar or less and the temperature is stable to within ± 0.01 K. The time necessary to attain equilibrium is at least 2 hours and for as long as 12 hours depending on the viscosity and quantity of ionic liquid.

The experimental mole fraction solubility results (x_2) were used to calculate the Henry's law constants (K_H / Pa) reported in Table S7 together with the mole fraction solubilities calculated at a partial pressure of gas equal to 0.1 MPa. The raw experimental solubility data was fitted as a function of temperature (T / K) by an empirical equation of the type:

$$\ln \left[K_H(T)(10^5 \text{ Pa}) \right] = \sum_{i=0}^n A_i (T(\text{K}))^{-i} \quad (\text{eq. S3})$$

the coefficients A_i obtained are listed in Table S8 together with the average relative deviations obtained for each IL solvent. These values can be regarded as an estimation of the precision of the experimental data which is in the present case always better or of the order of 1%. A representation of the experimental solubility (expressed as molar fraction) as a function of the different experimental temperatures studied is provided in Figure S20 and Figure S21. In Figure S20 is represented the solubility of argon in ionic

liquids constituted by [NTf₂]⁻ anion and different cations. In Figure S21 is represented the solubility of argon in ionic liquids constituted by the cations [(SiCSiC)C₁im]⁺ and [(SiOSiC)C₁im]⁺ and the anions [NTf₂]⁻, [N(CN)₂]⁻ and [B(CN)₄]⁻.

Table S7. Experimental values obtained for the solubility of argon in different pure ionic liquids, expressed both as Henry's law constants, K_H , and as argon mole fraction^a, x_2 .

T (K)	p (10 ² Pa) ^b	$x_{2,\text{exp}}$ (10 ⁻⁴) ^a	K_H (10 ⁵ Pa)	$x_{2, 0.1 \text{ MPa}}$ (10 ⁻⁴) ^a	Dev. (%) ^c
[C₈C₁im][NTf₂]					
308.32	698.36	18.0	387.79	25.8	+0.11
313.29	709.40	17.0	416.16	24.0	-0.17
323.21	731.50	14.7	498.42	20.1	+0.06
[(Np)C₁im][NTf₂]					
305.34	684.69	14.8	462.78	21.6	+0.37
308.32	672.37	14.6	459.52	21.8	-0.51
313.28	702.27	13.4	522.63	19.1	+0.32
315.75	688.32	13.3	517.59	19.3	-0.44
318.23	713.22	12.6	563.76	17.7	+0.33
320.71	698.94	12.5	558.14	17.9	-0.40
323.70	725.29	11.8	614.71	16.3	+0.44
328.15	714.85	11.3	631.87	15.8	-0.12
[(Me₄C₅)C₁im][NTf₂]					
305.61	744.04	21.3	348.91	28.6	+0.28
310.31	755.40	19.5	386.54	25.9	-0.10
313.28	762.60	18.3	416.99	24.0	-0.12
316.25	769.77	17.2	446.29	22.4	-0.25
320.21	779.39	15.3	508.25	19.7	+0.26
323.18	748.59	14.3	523.78	19.1	-0.41
323.19	777.97	14.4	541.50	18.5	+0.11
323.19	786.56	14.5	543.20	18.4	+0.16
343.00	794.21	9.4	847.51	11.8	+0.07
[(SiC)C₁im][NTf₂]					
303.39	662.69	15.5	427.11	23.4	+0.04
308.33	698.15	14.3	488.47	20.5	+0.65
310.81	701.90	14.4	485.91	20.6	-0.21
313.29	709.17	13.6	522.97	19.1	+0.22
313.30	683.81	14.0	489.84	20.4	-0.83
315.76	712.92	13.4	530.64	18.8	-0.27
318.23	720.26	12.3	583.88	17.1	+0.53
320.71	723.89	12.6	572.93	17.4	-0.47
323.19	731.27	11.6	632.59	15.8	+0.39
328.15	742.17	11.3	657.86	15.2	-0.33
333.12	753.28	10.1	744.08	13.4	+0.28

T (K)	p (10^2 Pa) ^b	$x_{2,\text{exp}}$ (10^{-4}) ^a	K_H (10^5 Pa)	$x_{2, 0.1 \text{ MPa}}$ (10^{-4}) ^a	Dev. (%) ^c
[(SiCSiC)C_{1im}][NTf₂]					
303.37	732.06	20.6	355.97	28.1	+1.80
308.33	690.67	20.8	331.31	30.2	-0.97
308.35	591.58	17.9	330.86	30.2	-1.00
313.29	755.41	19.3	392.15	25.5	+0.42
313.39	692.04	18.0	385.04	26.0	+0.09
315.77	707.06	18.9	373.36	26.8	-1.10
318.25	610.27	14.3	425.50	23.5	+0.38
323.21	723.48	16.7	432.60	23.1	-0.68
328.16	628.89	11.3	557.83	17.9	+2.16
328.17	734.43	15.1	486.03	20.6	-0.06
328.30	724.76	15.8	458.82	21.8	-1.03
[(SiCSiC)C_{1im}][B(CN)₄]					
303.37	695.76	15.2	457.19	21.9	+0.46
303.38	683.04	14.8	460.58	21.7	+0.58
308.33	694.01	14.1	492.94	20.3	+0.38
313.28	718.02	14.3	503.09	19.9	-0.54
318.25	715.84	13.3	540.05	18.5	-0.61
323.21	726.81	12.6	576.62	17.3	-0.72
328.15	751.52	12.1	621.41	16.1	-0.64
333.13	748.84	10.8	694.53	14.4	+0.01
338.07	773.90	10.4	741.01	13.5	-0.01
343.06	770.83	9.0	851.64	11.7	+1.10
[(SiCSiC)C_{1im}][N(CN)₂]					
307.14	646.80	7.8	827.44	12.1	+0.74
311.40	655.71	7.3	897.23	11.1	+0.40
313.25	775.21	8.4	922.94	10.8	+0.17
313.27	623.55	7.7	804.90	12.4	-1.84
313.40	659.79	7.5	877.36	11.4	-0.62
316.38	666.03	7.1	937.67	10.7	-0.65
320.34	674.38	6.3	1062.96	9.4	-0.15
323.18	799.51	6.0	1327.15	7.5	+2.11
323.18	643.22	5.0	1282.95	7.8	+1.63
323.32	680.59	6.1	1113.97	9.0	-0.42
326.30	686.81	5.8	1188.95	8.4	-0.42
328.17	753.35	5.9	1272.70	7.9	-0.03
333.27	701.30	5.3	1328.28	7.5	-0.92
[(SiOSiC)C_{1im}][NTf₂]					
313.27	685.40	19.2	356.33	28.1	+0.34
318.22	696.23	18.0	387.72	25.8	+0.05
318.23	778.06	19.8	392.94	25.4	+0.27
323.17	707.03	16.9	419.14	23.8	-0.28
323.18	790.11	18.3	431.17	23.2	+0.18
328.12	717.86	15.6	458.80	21.8	-0.36

T (K)	p (10^2 Pa) ^b	$x_{2,\text{exp}}$ (10^{-4}) ^a	K_{H} (10^5 Pa)	$x_{2, 0.1 \text{ MPa}}$ (10^{-4}) ^a	Dev. (%) ^c
328.14	802.13	17.2	465.93	21.5	-0.11
333.07	728.71	14.3	508.72	19.7	-0.18
333.11	814.11	16.4	496.62	20.1	-0.57
338.02	739.47	13.4	551.79	18.1	-0.31
342.96	750.29	12.1	622.50	16.1	+0.22
343.01	838.31	13.0	645.02	15.5	+0.76
[(SiOSiC)C _{1im}][B(CN) ₄]					
303.38	710.90	16.9	419.52	23.8	+0.35
313.29	733.68	15.5	472.54	21.2	-0.38
318.26	748.65	14.6	512.36	19.5	-0.33
320.74	754.47	13.8	545.54	18.3	+0.06
323.20	756.56	13.4	563.54	17.7	-0.01
328.17	771.67	12.4	619.89	16.1	+0.33

^a $x_{2, \text{exp}}$ is the argon molar fraction obtained in equilibrium at the experimental conditions;

$x_{2, 0.1 \text{ MPa}}$ is the argon molar fraction corrected for a partial pressure of solute of 0.1 MPa;

^b p is the experimental equilibrium pressure; ^c Dev. is the percent deviation of the experimental data relatively to the correlations reported in Table S7.

Table S8. Parameters of eq. S3 used to fit the experimental results presented in Table S7, expressed on K_{H} , along with the per cent average relative deviation of the fit (ARD)

IL	A_0	A_1	ARD (%)
[C ₈ C _{1im}][NTf ₂]	11.47 ± 0.38	- 1701 ± 118	± 0.11
[(Np)C _{1im}][NTf ₂]	11.03 ± 0.43	- 1502 ± 137	± 0.37
[(Me ₄ C ₅)C _{1im}][NTf ₂]	14.09 ± 0.17	- 2521 ± 54	± 0.20
[(SiC)C _{1im}][NTf ₂]	12.09 ± 0.35	- 1831 ± 112	± 0.38
[(SiCSiC)C _{1im}][NTf ₂]	11.32 ± 0.82	- 1684 ± 259	± 0.88
[(SiCSiC)C _{1im}][B(CN) ₄]	11.08 ± 0.32	- 1513 ± 103	± 0.50
[(SiCSiC)C _{1im}][N(CN) ₂]	14.19 ± 0.93	- 2310 ± 297	± 0.78
[(SiOSiC)C _{1im}][NTf ₂]	12.37 ± 0.25	- 2040 ± 81	± 0.30
[(SiOSiC)C _{1im}][B(CN) ₄]	11.18 ± 0.35	- 1567 ± 111	± 0.24

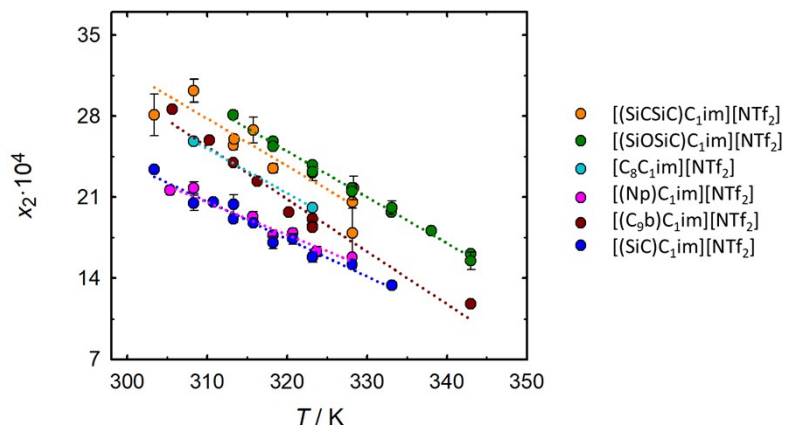


Figure S20. Mole fraction gas solubility of argon in [cation][NTf₂] ionic liquids at 0.1MPa partial pressure of the solute and as a function of temperature. The lines are just a guide to the eye.

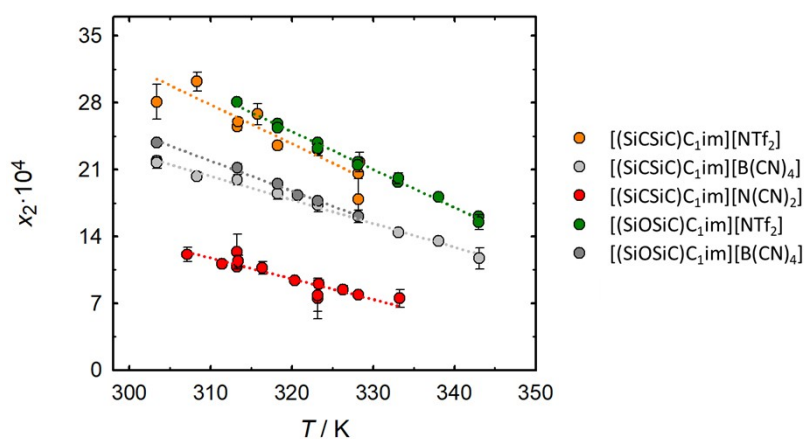


Figure S21. Mole fraction gas solubility of argon in ionic liquids constituted by the cations [(SiCSiC)C₁im]⁺ and [(SiOSiC)C₁im]⁺ and the anions [NTf₂]⁻, [N(CN)₂]⁻ and [B(CN)₄]⁻, at 0.1MPa partial pressure of the solute and as a function of temperature. The lines are just a guide to the eye.

11. Thermodynamic properties derived from gas solubility measurements

Given the experimental low pressure of the argon solute, the thermodynamic properties of solvation were derived from the variation of the solubility (expressed in Henry's law constant) with temperature. The Gibbs energy of solvation of the argon at infinite dilution in the different ionic liquids studied is presented in Table S9 for the temperatures studied in this project. Together with the Gibbs energy of solvation, the enthalpy and entropy of solvation are also presented. In Figure S22 and Figure S23 the enthalpy and entropy of solvation of argon at infinite dilution are presented as a function of the temperature. In Figure S22 are represented the thermodynamic properties enthalpy and entropy regarding the solvation of argon in ionic liquids constituted by $[\text{NTf}_2]^-$ anion and different cations. In Figure S23 are represented the thermodynamic properties enthalpy and entropy regarding the solvation of argon in ionic liquids constituted by the cations $[(\text{SiCSiC})\text{C}_1\text{im}]^+$ and $[(\text{SiOSiC})\text{C}_1\text{im}]^+$ and the anions $[\text{NTf}_2]^-$, $[\text{N}(\text{CN})_2]^-$ and $[\text{B}(\text{CN})_4]^-$.

Table S9. Thermodynamic functions of solvation of argon in the studied ionic liquids

T (K)	$\Delta_{\text{sol}}G^\infty$ ($\text{kJ}\cdot\text{mol}^{-1}$) ^a	$\Delta_{\text{sol}}H^\infty$ ($\text{kJ}\cdot\text{mol}^{-1}$) ^b	$\Delta_{\text{sol}}S^\infty$ ($\text{J}\cdot\text{mol}^{-1}\cdot\text{K}^{-1}$) ^c
$[\text{C}_8\text{C}_1\text{im}][\text{NTf}_2]$			
308.32	15.28	-13	-93
313.29	15.71	-14	-95
323.21	16.69	-15	-97
Uncertainty	± 0.03	± 2	± 5
$[(\text{Np})\text{C}_1\text{im}][\text{NTf}_2]$			
305.34	15.6	-12	-89
308.32	15.7	-12	-90
313.28	16.3	-12	-91
315.75	16.4	-12	-92
318.23	16.8	-13	-92
320.71	16.9	-13	-93
323.70	17.3	-13	-94
328.15	17.6	-13	-95
Uncertainty	± 0.1	± 2	± 7
$[(\text{Me}_4\text{C}_5)\text{C}_1\text{im}][\text{NTf}_2]$			
305.61	14.88	-18.7	-110
310.31	15.37	-19.2	-112
313.28	15.71	-19.6	-113
316.25	16.04	-20.0	-114
320.21	16.59	-20.5	-116
323.18	16.82	-20.9	-117
323.19	16.91	-20.9	-117

T (K)	$\Delta_{\text{sol}}G^{\infty}$ (kJ·mol ⁻¹) ^a	$\Delta_{\text{sol}}H^{\infty}$ (kJ·mol ⁻¹) ^b	$\Delta_{\text{sol}}S^{\infty}$ (J·mol ⁻¹ ·K ⁻¹) ^c
323.19	16.92	-20.9	-117
343.00	19.23	-23.5	-125
Uncertainty	± 0.07	± 0.9	± 3
[(SiC)C₁im][NTf₂]			
303.39	15.3	-14	-96
308.33	15.9	-14	-98
310.81	16.0	-15	-98
313.29	16.3	-15	-99
313.30	16.1	-15	-99
315.76	16.5	-15	-100
318.23	16.9	-15	-101
320.71	16.9	-15	-101
323.19	17.3	-16	-102
328.15	17.7	-16	-104
333.12	18.3	-17	-105
Uncertainty	± 0.1	± 2	± 6
[(SiCSiC)C₁im][NTf₂]			
303.37	14.8	-13	-90
308.33	14.9	-13	-92
308.35	14.9	-13	-92
313.29	15.6	-14	-93
313.39	15.5	-14	-93
315.77	15.5	-14	-94
318.25	16.0	-14	-95
323.21	16.3	-15	-96
328.16	17.3	-15	-97
328.17	16.9	-15	-97
328.30	16.7	-15	-97
Uncertainty	± 0.3	± 4	± 13
[(SiCSiC)C₁im][B(CN)₄]			
303.37	15.4	-11	-88
303.38	15.5	-11	-88
308.33	15.9	-12	-89
313.28	16.2	-12	-90
318.25	16.6	-12	-92
323.21	17.1	-13	-93
328.15	17.5	-13	-94
333.13	18.1	-14	-95
338.07	18.6	-14	-96
343.06	19.2	-14	-97
Uncertainty	± 0.2	± 1	± 4
[(SiCSiC)C₁im][N(CN)₂]			
307.14	17.2	-18	-113
311.40	17.6	-18	-115

T (K)	$\Delta_{\text{sol}}G^{\infty}$ (kJ·mol ⁻¹) ^a	$\Delta_{\text{sol}}H^{\infty}$ (kJ·mol ⁻¹) ^b	$\Delta_{\text{sol}}S^{\infty}$ (J·mol ⁻¹ ·K ⁻¹) ^c
313.25	17.8	-18	-115
313.27	17.4	-18	-115
313.40	17.7	-18	-115
316.38	18.0	-19	-117
320.34	18.6	-19	-118
323.18	19.3	-20	-119
323.18	19.2	-20	-119
323.32	18.9	-20	-119
326.30	19.2	-20	-120
328.17	19.5	-20	-121
333.27	19.9	-21	-123
Uncertainty	± 0.3	± 5	± 16
[(SiOSiC)C_{1im}][NTf₂]			
313.27	15.30	-15	-98
318.22	15.77	-16	-100
318.23	15.81	-16	-100
323.17	16.22	-16	-101
323.18	16.30	-16	-101
328.12	16.72	-17	-103
328.14	16.76	-17	-103
333.07	17.26	-17	-104
333.11	17.19	-17	-104
338.02	17.74	-18	-106
342.96	18.35	-19	-107
343.01	18.45	-19	-107
Uncertainty	± 0.08	± 1	± 4
[(SiOSiC)C_{1im}][B(CN)₄]			
303.38	15.23	-12	-90
313.29	16.04	-13	-93
318.26	16.51	-13	-94
320.74	16.81	-14	-95
323.20	17.02	-14	-95
328.17	17.54	-14	-96
Uncertainty	± 0.07	± 2	± 5

^a The uncertainty of the Gibbs free energy of solvation is an estimation of the confidence interval at a confidence level of 95% ($\pm 2 \cdot \sigma$), reflecting the dispersion of the experimental results; ^b The uncertainty of the enthalpy of solvation is an estimation of the confidence interval at a confidence level of 95%, reflecting the propagation of the uncertainty associated to the derivative of the Gibbs energy of solvation and precision of temperature measurements; ^c The uncertainty of the entropy of solvation is an estimation of the confidence interval at a confidence level of 95%, reflecting the propagation of the uncertainty associated to the Gibbs energy of solvation, the enthalpy of solvation and precision of temperature measurements.

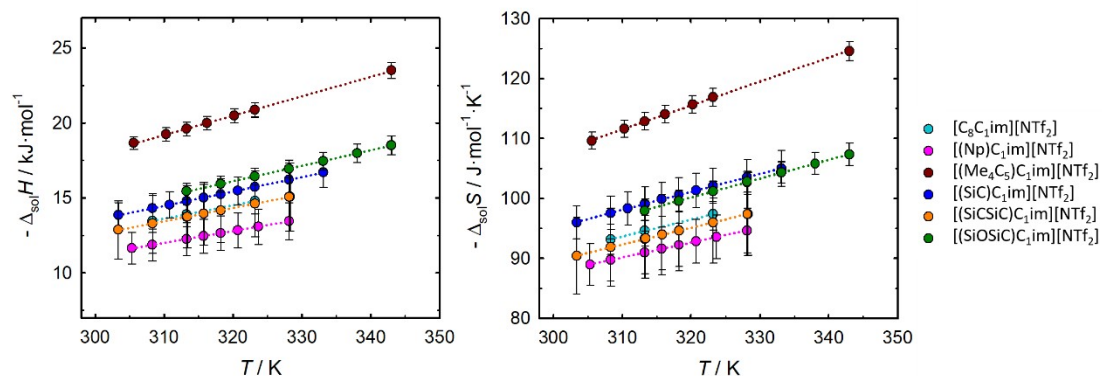


Figure S22. Molar enthalpy (left) and entropy (right) of solvation of argon at infinite dilution in $[\text{cation}][\text{NTf}_2]$ ionic liquids, as a function of temperature. The lines are just a guide to the eye.

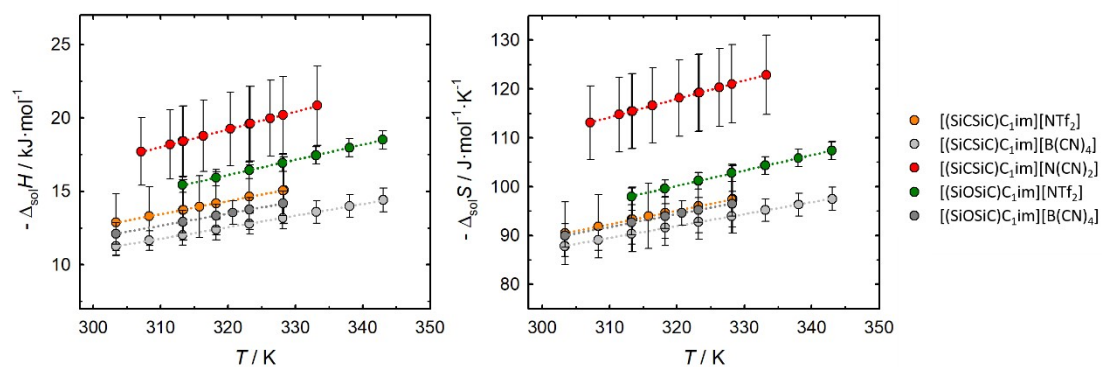


Figure S23. Molar enthalpy (left) and entropy (right) of solvation of argon at infinite dilution in ionic liquids constituted by the cations $[(\text{SiCSiC})\text{C}_1\text{im}]^+$ and $[(\text{SiOSiC})\text{C}_1\text{im}]^+$ and the anions $[\text{NTf}_2]^-$, $[\text{N}(\text{CN})_2]^-$ and $[\text{B}(\text{CN})_4]^-$, as a function of temperature. The lines are just a guide to the eye.

12. Correlation between argon solubility and molar volume of ionic liquids

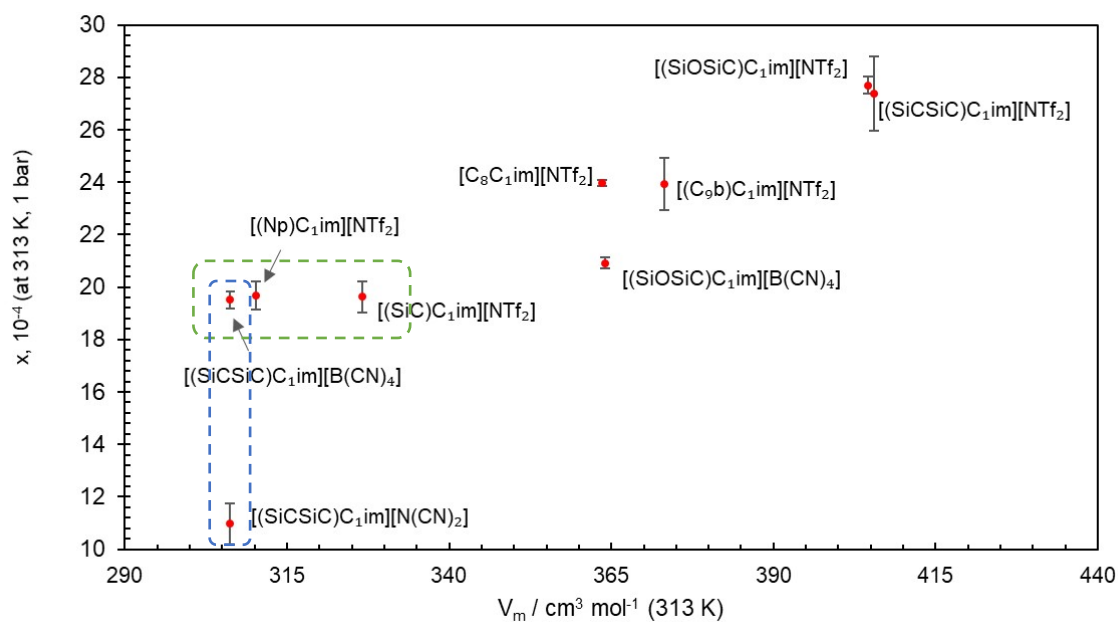


Figure S24. Measured argon solubility vs. molar volume of the ionic liquid at 313 K.

13. List of ionic liquid intermediates prepared according to paths A or B

Table S10

Ionic liquid intermediates $[RC_1im]X$ prepared in this study, synthetic paths according to Figure 1, melting points and crystallization solvents.

No	Cation	X^-	Path	m.p. ^a / °C	solvent
1	$[[C_8C_1im]^+$	Br^-	A	n.d.	-
2	$[(Np)C_1im]^+$	TsO^-	B	121-124	EtOAc
3	$[(Me_4C_5)C_1im]^+$	TsO^-	B	n.d.	EtOAc
4	$[(SiC)C_1im]^+$	I^-	B	84-86	EtOAc
5	$[(SiCSiC)C_1im]^+$	Cl^-	A	69-71	Me_2CO
6	$[(SiCSiSiC)C_1im]^+$	Cl^-	A	69-71	Me_2CO
7	$[(SiOSiC)C_1im]^+$	Cl^-	A	141-143	MeCN

^a determined using the melting point apparatus

14. Synthetic approaches for introduction of cation side-chains and anion metathesis

The branched C₉-side-chain in [(Me₄C₅)C₁im]⁺ was first introduced in the neutral imidazole, following a six-step route (**Figure S25**). To begin, a commercially available alkene **3** was hydrochlorinated to yield the tertiary chloroalkane **4**. An extension by one carbon atom within the back-bone was required, which was achieved by preparing the Grignard reagent **5** and subsequently reacting it with CO₂ to afford the branched carboxylic acid **6**. The acid was then converted into the alcohol **7** via borane reduction, and the obtained alcohol treated with methanesulfonyl chloride to yield the mesylate **8**. This branched mesylate ester was found to be a suitable alkylating agent for sodium imidazolidate in preparation of the alkylimidazole **9**. Despite a high reactivity was expected for **8** with Na[im], elevated temperature was required, as the non-polar **8** would otherwise not be soluble in the reaction medium. A similar salting-out effect was observed during the preparation of 1-(neopentyl)imidazole.

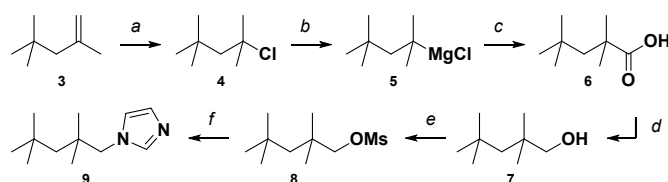


Figure S25. Preparative route of the branched alkylimidazole. Reaction conditions: *a* – HCl gas, Et₂O, 0 °C, 3 h, 84%; *b* – Mg, EtBr, Et₂O, 35 °C, 3 h; *c* – CO₂ gas, 0 °C, 2 h, 21%; *d* – BH₃·THF, 65 °C, 3 h, HCl, 70%; *e* – MsCl, Et₃N, DCM, 0 °C, 2.5 h, 82%; *f* – Na[im], DMSO, 115 °C, 16 h, 88%.

Chloroalkylsilanes were another important group of precursors for homologous IL series comprising silicon atoms. Chlormethyldimethylchlorosilane **15** was used as a commercially available key building-block. In presence of the Grignard reagent **11** or silanolate **14**, a rapid and selective reaction at the Si centre was observed, preserving the chloromethyl moiety. A further silane chain elongation from two Si atoms to three could be carried out similarly as in preparation of **12**.

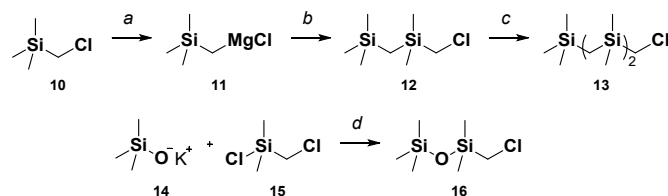
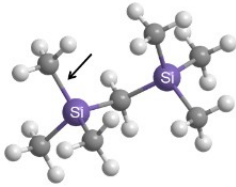
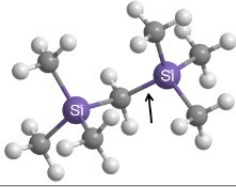
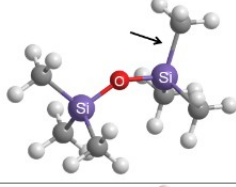
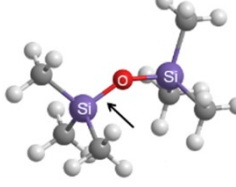
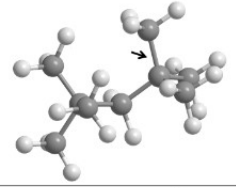
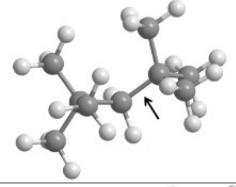
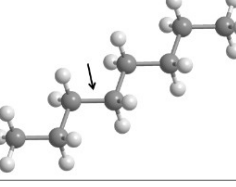


Figure S25. Preparative routes of chloromethylsilanes. Reaction conditions: *a* – Mg, THF, 65 °C; *b* – ClSi(Me₂)CH₂Cl **13**, THF, 65 °C, 24 h, 90%; *c* – Mg, THF, unstirred, then ClSi(Me₂)CH₂Cl, THF, 65 °C, 24 h, 84%.

The last step towards final ILs (**Table 1** in the manuscript) was the anion metathesis for the obtained intermediates (**Table S10**). Thanks to its well-known hydrophobic nature, ILs comprising *bis*-(trifluoromethanesulfonyl)imide anion [NTf₂]⁻ could be prepared in high yields using aqueous precursor solutions and the DCM extraction. Similar approach was utilized for [B(CN)₄]⁻ ILs and much to our surprise, it was found to be suitable for the rather hydrophilic [N(CN)₂]⁻ ILs as well. We associate this with the non-polar nature of imidazolium cations used herein. Combined with the charge-diffuse nature of [N(CN)₂]⁻, the ion pairs are hydrophobic enough to prefer the organic solvent phase. This is a rather feasible, as dicyanamide-based ILs are routinely obtained using the corresponding silver salt.

15. Bond lengths in hydrocarbons and their silicon analogue molecules

Table S11. Bond lengths from crystal structures of molecular analogues of the listed molecules, extracted from Cambridge Crystallography database using *CCDC Mogul* software. Bond lengths obtained using molecular mechanics (MM2) in Chem3D Pro by CambridgeSoft shown in parentheses

Bond searched	Hits in CCDC <i>Mogul</i> search	Avg bond length (MM bond length)
	1033	1.87±0.03 Å (1.88 Å)
	99	1.87±0.02 Å (1.88 Å)
	6617	1.85±0.04 Å (1.88 Å)
	472	1.62±0.03 Å (1.63 Å)
	10191	1.52±0.03 Å (1.53 Å)
	658	1.55±0.03 Å (1.55 Å)
	12569	1.51±0.05 Å (1.54 Å)

16. Molar volume of ionic liquids

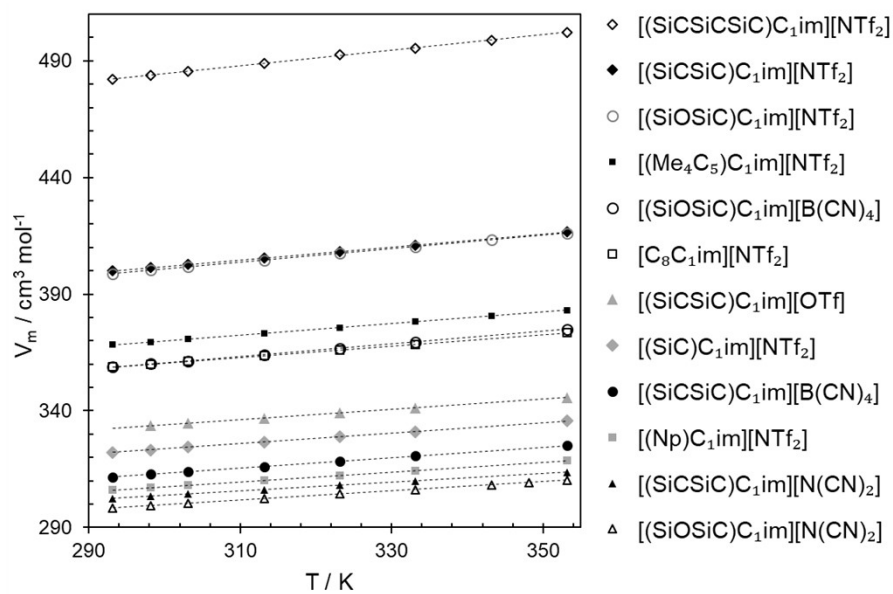


Figure S26. Molar volume (V_m) of the studied ILs as a function of temperature (T).

References

- 1 S. Plimpton, *J. Comput. Phys.*, 1995, **117**, 1–19.
- 2 A. Dequidt, J. Devémy and A. A. H. Pádua, *J. Chem. Inf. Model.*, 2016, **56**, 260–268.
- 3 L. Martínez, R. Andrade, E. G. Birgin and J. M. Martínez, *J. Comput. Chem.*, 2009, **30**, 2157–2164.
- 4 A. A. H. Padua, *fftool*, <https://github.com/paduagroup/fftool>.
- 5 K. Goloviznina and A. A. H. Padua, *clandpol*, <https://github.com/paduagroup/clandpol>.
- 6 C. Y. Son, J. G. McDaniel, Q. Cui and A. Yethiraj, *J. Phys. Chem. Lett.*, 2019, **10**, 7523–7530.
- 7 K. Goloviznina, Z. Gong, M. F. Costa Gomes and A. A. H. Pádua, *J. Chem. Theory Comput.*, 2021, **17**, 1606–1617.
- 8 G. Lamoureux and B. Roux, *J. Chem. Phys.*, 2003, **119**, 3025–3039.
- 9 E. Heid, A. Szabadi and C. Schröder, *Phys. Chem. Chem. Phys.*, 2018, **20**, 10992–10996.
- 10 P. Schwerdtfeger and J. K. Nagle, *Mol. Phys.*, 2019, **117**, 1200–1225.
- 11 C. E. S. Bernardes, K. Shimizu, J. N. C. Lopes, P. Marquetand, E. Heid, O. Steinhauser and C. Schröder, *Phys. Chem. Chem. Phys.*, 2016, **18**, 1665–1670.
- 12 B. T. Thole, *Chem. Phys.*, 1981, **59**, 341–350.
- 13 S. Y. Noskov, G. Lamoureux and B. Roux, *J. Phys. Chem. B*, 2005, **109**, 6705–6713.
- 14 K. Goloviznina, J. N. Canongia Lopes, M. Costa Gomes and A. A. H. Pádua, *J. Chem. Theory Comput.*, 2019, **15**, 5858–5871.
- 15 K. Goloviznina, Z. Gong and A. A. H. Padua, *Wiley Interdiscip. Rev. Comput. Mol. Sci.*, DOI:10.1002/wcms.1572.
- 16 B. Wu, H. Shirota, S. Lall-Ramnarine and E. W. Castner, *J. Chem. Phys.*, 2016, **145**, 114501.
- 17 C. M. Breneman and K. B. Wiberg, *J. Comput. Chem.*, 1990, **11**, 361–373.
- 18 M. J. Frisch, G. W. Trucks, H. B. Schlegel, G. E. Scuseria, M. A. Robb, J. R. Cheeseman, G. Scalmani, V. Barone, G. A. Petersson, H. Nakatsuji, X. Li, M. Caricato, A. V. Marenich, J. Bloino, B. G. Janesko, R. Gomperts, B. Mennucci, H. P. Hratchian, J. V. Ortiz, A. F. Izmaylov, J. L. Sonnenberg, D. Williams-Young, F. Ding, F. Lipparini, F. Egidi, J. Goings, B. Peng, A. Petrone, T. Henderson, D. Ranasinghe, V. G. Zakrzewski, J. Gao, N. Rega, G. Zheng, W. Liang, M. Hada, M. Ehara, K. Toyota, R. Fukuda, J. Hasegawa, M. Ishida, T. Nakajima, Y. Honda, O. Kitao, H. Nakai, T. Vreven, K. Throssell, J. Montgomery, J. A., J. E. Peralta, F. Ogliaro, M. J. Bearpark, J. J. Heyd, E. N. Brothers, K. N. Kudin, V. N. Staroverov, T. A. Keith, R. Kobayashi, J. Normand, K. Raghavachari, A. P. Rendell, J. C. Burant, S. S. Iyengar, J. Tomasi, M. Cossi, J. M. Millam, M. Klene, C. Adamo, R. Cammi, J. W. Ochterski, R. L. Martin, K. Morokuma, O. Farkas, J. B. Foresman and D. J. Fox, *Gaussian 16*.
- 19 E. K. Watkins and W. L. Jorgensen, *J. Phys. Chem. A*, 2001, **105**, 4118–4125.
- 20 J. N. Canongia Lopes and A. Pádua, *Theor. Chem. Acc.*, 2012, **131**, 1129.
- 21 W. L. Jorgensen, D. S. Maxwell and J. Tirado-Rives, *J. Am. Chem. Soc.*, 1996, **118**, 11225–11236.
- 22 A. A. H. Pádua, *J. Chem. Phys.*, 2017, **146**, 204501.

- 23 B. Hess, *J. Chem. Phys.*, 2001, **116**, 209–217.
- 24 M. Brehm and B. Kirchner, *J. Chem. Inf. Model.*, 2011, **51**, 2007–2023.
- 25 S. Gehrke, R. Macchieraldo and B. Kirchner, *Phys. Chem. Chem. Phys.*, 2019, **21**, 4988–4997.
- 26 M. Brehm, M. Thomas, S. Gehrke and B. Kirchner, *J. Chem. Phys.*, 2020, **152**, 164105.
- 27 T. C. Beutler, A. E. Mark, R. C. van Schaik, P. R. Gerber and W. F. van Gunsteren, *Chem. Phys. Lett.*, 1994, **222**, 529–539.
- 28 H. E. Gottlieb, V. Kotlyar and A. Nudelman, *J. Org. Chem.*, 1997, **62**, 7512–7515.
- 29 F. Philippi, D. Rauber, B. Kuttich, T. Kraus, C. W. M. Kay, R. Hempelmann, P. A. Hunt and T. Welton, *Phys. Chem. Chem. Phys.*, 2020, **22**, 23038–23056.
- 30 M. A. Ab Rani, A. Brant, L. Crowhurst, A. Dolan, M. Lui, N. H. Hassan, J. P. Hallett, P. A. Hunt, H. Niedermeyer, J. M. Perez-Arlandis, M. Schrems, T. Welton and R. Wilding, *Phys. Chem. Chem. Phys.*, 2011, **13**, 16831.
- 31 D. Antoniak and M. Barbasiewicz, *Org. Lett.*, 2019, **21**, 9320–9325.
- 32 E. Bakis, A. van den Bruinhorst, L. Pison, I. Palazzo, T. Chang, M. Kjellberg, C. C. Weber, M. Costa Gomes and T. Welton, *Phys. Chem. Chem. Phys.*, 2021, **23**, 4624–4635.
- 33 T. Maji, K. Tsimenidis, R. Nagarajan, R. Mosurkal, J. Kumar and M. Gkikas, *Polymer (Guildf.)*, 2020, **197**, 122487.
- 34 F. Whitmore, W. Wheeler and J. Surmatis, *J. Am. Chem. Soc.*, 1941, **63**, 3237–3237.
- 35 M. Kawashima, T. Sato and T. Fujisawa, *Tetrahedron*, 1989, **45**, 403–412.
- 36 R. DiCosimo, S. S. Moore, A. F. Sowinski and G. M. Whitesides, *J. Am. Chem. Soc.*, 1982, **104**, 124–133.
- 37 E. Westphal, H. Gallardo, G. F. Caramori, N. Sebastián, M.-G. Tamba, A. Eremin, S. Kawauchi, M. Prehm and C. Tschierske, *Chem. - A Eur. J.*, 2016, **22**, 8181–8197.
- 38 H. Shirota, J. F. Wishart and E. W. Castner, *J. Phys. Chem. B*, 2007, **111**, 4819–4829.
- 39 L. C. Tomé, A. S. L. Gouveia, M. A. Ab Rani, P. D. Lickiss, T. Welton and I. M. Marrucho, *Ind. Eng. Chem. Res.*, 2017, **56**, 2229–2239.
- 40 S. Bulut, M. A. Ab Rani, T. Welton, P. D. Lickiss and I. Krossing, *ChemPhysChem*, 2012, **13**, 1802–1805.
- 41 T. Endo, S. Nemugaki, Y. Matsushita, Y. Sakai, H. Ozaki, Y. Hiejima, Y. Kimura and K. Takahashi, *Chem. Phys.*, 2016, **472**, 128–134.